5-15-2002

A Finite-Element Model of Basal Water Generated by Melting in an Ice Sheet Model

James L. Fastook

Principal Investigator; University of Maine, Orono, fastook@maine.edu

Final Report for Period: 03/1999 - 02/2002 **Submitted on:** 05/15/2002
Principal Investigator: Fastook, James L.
Award ID: 9873556
Organization: University of Maine
Title:
A Finite-Element Model of Basal Water Generated by Melting in an Ice Sheet Model

Project Participants

Senior Personnel

Name: Fastook, James

Worked for more than 160 Hours: Yes

Contribution to Project:

Dr. Fastook is overseeing the modification of his ice sheet model to incorporate the movement of basal water, produced by melting at the bed.

Name: Tulaczyk, Slawek

Worked for more than 160 Hours: Yes

Contribution to Project:

Dr. Tulaczyk's role in this work with Dr. Fastook of the University of Maine at Orono is as a subcontracted expert in ice-sheet hydrology. He is analyzing the existing observational and theoretical constraints on subglacial water flow to provide realistic parameters and laws for treatment of sub-ice-sheet hydrology in Dr. Fastook's finite-element model of the Antarctic ice sheet.

Post-doc

Name: Khatwa, Anjana

Worked for more than 160 Hours: Yes

Contribution to Project:

Dr. Anjana Khatwa assisted ST in performing new research on this problem. ST worked on development of a new analytical drainage model in a soft-bed environment and AK collected new observational evidence useful in constraining the model. Her work concentrated on using modern samples of sub-ice stream till from West Antarctica as well as samples of Late Pleistocene deforming-bed tills from UK.

Graduate Student

Name: Johnson, Jesse

Worked for more than 160 Hours: Yes

Contribution to Project:

Jesse Johnson is a PhD candidate in the Physics Department here at the University of Maine. His thesis topic involves the implementation of the water model developed by this grant.

Undergraduate Student

Other Participant

Research Experience for Undergraduates

Organizational Partners

University of Kentucky

Dr. Tulaczyk, at the University of Kentucky, is participating as a subcontractor for this grant.

Other Collaborators or Contacts

Activities and Findings

Research and Education Activities: (See PDF version submitted by PI at the end of the report)

A meeting held in Maine the summer of 1999, attended by Fastook (JLF), Tulaczyk (ST), and Johnson (JJ) involved working through the various possible mechanisms whereby water could move at the bed. This meeting was the basis for all subsequent work, both by JF's group and by ST's group. Dr. Anjana Khatwa (AK) joined ST's group when he moved from Kentucky to California.

JF's group:

A major accomplishment was the development of an algorithm for predicting the positions of Antarctic lakes. This work is the subject of a paper submitted to the Journal of Glaciology ('Predicting the Locations of Lakes beneath Antarctica,' by James L. Fastook and Jesse Johnson, submitted to J. Glaciology 13 March 2002). JJ also looked at the lakes as a potential source of water for fast-flowing ice streams. This will be presented at the International Symposium on Fast Glacier Flow Yakutat, Alaska, U.S.A., 10-14 June 2002, and will eventually be published in the Annals of Glaciology.

The ice sheet model, with its new basal water component, was also applied to paleo-ice sheets and presented at the INCEPTIONS Workshop held in June 2001 in Sweden. The paper, 'Northern Hemisphere Glaciation and its Sensitivity to Basal Melt Water,' by Jesse V. Johnson and James L. Fastook has been accepted for publication in The INCEPTIONS Proceedings in Quaternary International.

Results have also been presented at regular WAIS meetings held in September of each year in Washington, DC.

A complete description of the University of Maine Ice Sheet Model (UMISM) is included as a pdf attachment.

ST's group:

ST focused on compilation of existing mathematical models of subglacial drainage and performed an intercomparison of these models. The primary goal was to simplify the various mathematical models into a few formulas that can be realistically implemented into a numerical ice-sheet model. There were several basic challenges that had to be overcome in order to achieve this goal. These are addressed below.

All of the existing basal drainage formulas were developed based on experimental and/or theoretical analyses of small drainage systems, lengthscales of the order of 0.1-10 m) whereas the numerical ice-sheet model operates with individual elements representing lengthscales of the order of 10,000 m. Hence, a method for spatial extrapolation and averaging of basal drainage characteristics had to be devised. The method that was ultimately used invoked an estimate of the number of individual drainage elements (e.g., tunnels, channels) per unit area.

Another important limitation of the existing basal drainage models stemmed from the fact that they typically focus on expressing basal water drainage as a function of water/effective pressures and/or pressure gradients. However, pressure is not a conserved quantity that can be easily implemented into a numerical ice-sheet model, which is build around the requirement of mass (not pressure) conservation. Hence, it was necessary to reformulate the mathematical drainage models, so that the pressure terms were substituted by terms involving volumes of water stored in a given numerical element over a given time period.

One key aspect of sub-ice sheet drainage that is still poorly researched is the physical nature of water drainage over deformable till beds. AK assisted ST in performing new research on this problem. ST worked on development of a new analytical drainage model in a soft-bed environment and AK collected new observational evidence useful in constraining the model. Her work concentrated on using modern samples of sub-ice stream till from West Antarctica as well a samples of Late Pleistocene deforming-bed tills from UK.

Presentations

AK presented the results of her research sponsored by this subcontract at the 2000 West Antarctic Ice Sheet Workshop in Arlington, VA.

Dr. Slawek Tulaczyk is presenting the results of his research sponsored by this subcontract at the 2002 Fast Ice Flow Symposium sponsored by the International Glaciological Society.

Findings: (See PDF version submitted by PI at the end of the report)

The major finding of JF's group are included in an attached pdf. The pdf includes the abstract for JJ's thesis, his conclusion section, and his chapter 3, which is a detailed discussion of the basal water model, particularly its development and implementation.

Applications of the basal water model can be found in a paper submitted to the Journal of Glaciology ('Predicting the Locations of Lakes beneath Antarctica,' by James L. Fastook and Jesse Johnson, submitted to J. Glaciology 13 March 2002).

A paper looking at lakes as a potential source of water for fast-flowing ice streams will be presented at the International Symposium on Fast Glacier Flow Yakutat, Alaska, U.S.A., 10-14 June 2002, and will eventually be published in the Annals of Glaciology.

Another application to paleo-ice sheets was presented at the INCEPTIONS Workshop held in June 2001 in Sweden. The paper, 'Northern Hemisphere Glaciation and its Sensitivity to Basal Melt Water,' by Jesse V. Johnson and James L. Fastook has been accepted for publication in The INCEPTIONS Proceedings in Quaternary International.

Training and Development:

Jesse Johnson, a PhD candidate in the Physics Department at the University of Maine has been supported by this grant. His thesis involveed implementation of the water model developed by this grant. Thus far Jesse has given several talks on his involvement, one at an internal seminar series in the Institute for Quaternary Studies here at the University of Maine, anothers at the Annual WAIS Workshops, held in September, 1999 and 2000 in Sterling, VA, and another at the INCEPTIONS workshop, held in Sweden in June 2001.

He has also learned the Finite-Element Method, for application of this model. He has performed a number of experiments with the current University of Maine Ice Sheet Model (UMISM), to which he will be adding the hydrological model.

This subcontract provided part of a one-year postdoctoral fellowship for AK. This was the first post-Ph.D. appointment for her and provided her with an important advanced training opportunity. In the course of the postdoc she has broadened her research profile. AK has also published one peer-reviewed paper based partly on her work sponsored by this subcontract.

Outreach Activities:

I regularly give presentations to new students here at the University on 'Glaciology as a Computer Science Problem.' This involves motivating them as to why glaciology is worth studying (climate change, ice ages, CO2 warming, ice cores, etc.). I also meet with prospective students from Maine High Schools during their visits to the University campus.

Journal Publications

James L. Fastook and Jesse Johnson
, "Predicting the Locations of Lakes beneath Antarctica", Journal of Glaciology, p. , vol. , ( ). Submitted

Jesse V. Johnson and James L. Fastook, "Northern Hemisphere Glaciation and its Sensitivity to Basal Melt Water", Quaternary International , p. , vol. , ( ). Accepted

Jesse V. Johnson and James L. Fastook, "Lake instability mechanism for fast flow of ice streams", Annals of Glaciology, p. , vol. , ( ). Submitted

Khatwa, A. and S. Tulaczyk, "Microstructural interpretations of modern and
Quaternary subglacially deformed sediments: The relative role of parent material
and subglacial processes.", Journal of Quaternary Science, p. 507, vol. 16, (2001). Published

Books or Other One-time Publications

Jesse V. Johnson, "A Basal Water Model for Ice Sheets", (2002). Thesis, Accepted
Bibliography: A thesis submitted in partial requirement for the degree of Doctor of Philosophy (in physics), University of Maine, Orono, ME

Web/Internet Site

URL(s):

http://rose.umcs.maine.edu/~shamis/papers/pap.html

Description:

URL contains links to postscript and pdf copies of paper and accompanying slides for presentation at 1999 sixth annual WAIS conference held 15-18 September, 1999 in Sterling, VA.

Other Specific Products

Contributions

Contributions within Discipline:

Researchers in various areas develop theoretical frameworks within which they can interpret their experimental data. These theoretical frameworks, or models, incorporate as complete a description of the physical processes connecting different aspects of the experimental data as is possible. Comparison of the modeling results with the experimental data allows the researchers to verify their intuitions regarding the underlying physical processes that control the system being studied. A good model can be used in a predictive fashion to describe the behavior of a system subject to a different environment or at a different time in its evolution. Within the constraints of the theoretical framework, researchers can extend their vision beyond the measurable surface of the phenomenon, allowing them to literally 'see' inside the system which they are experimentally observing.

Physics-based modeling of this type is intrinsically dependent on the modern computer to make meaningful sense of the wealth of experimental data available for many fields of study. Traditionally modelers have used restrictive assumptions and simplified domains to allow for the analytic solution of the equations describing their physical system. With the advent of modern computers numerical methods which yield an approximate solution can be applied to equations which are not amenable to analytic evaluation, thereby allowing the researchers to solve the exact equations without restrictive assumptions or simplified domains.

Contributions to Other Disciplines:

Glacial modeling ties in intrinsically to many other disciplines, but is particularly important to the study of climate change. Predictions of future climate change depends on accurate interpretation of past climate change, and glaciers are seen as sensitive indicators of such change. In addition large ice sheets serve as repositories of past climate information in the form of deep ice cores. Interpretation of these ice cores depends on modeling for chronologies as well as other aspects of the core necessary to understand the preserved record.

Contributions to Human Resource Development:

Awareness of the impact of human behavior on the environment is important to instill in our young students. Study of the past in Antarctica gives us a window into the future. There are many unanswered and controversial questions about the ice sheets that will need to be solved to address the issue of human impact.

Contributions to Resources for Research and Education:

Results of ST's work on subglacial drainage have been incorporated into undergraduate and graduate courses that he teaches at UCSC (EART 148 and EART 290). Both courses are offered every other year with typical enrollment of 10 for the undergraduate one and 5 for the graduate one. ST's analyses of subglacial drainage have also facilitated his involvement in advising graduate students doing relevant research projects. This includes three of ST's own graduate students (Marion Bougamont, Ian Howat, and Stefan Vogel) who all work on topics incorporating some aspects of subglacial water drainage. ST has also acted as a M.Sc. thesis committee member for Erin Kraal, a graduate student of Drs. Robert and Suzanne Anderson. Erin Kraal's thesis focused on observations and modeling of annual outburst floods on Kennicot Glacier, Alaska.

Contributions Beyond Science and Engineering:

Ice sheet modeling is but one small component in our attempt to understand how the world climate system works. Policy makers need predictions so that they can plan for future contingencies. Models can make predictions which can be trusted only so much as the models can accurately describe the past and all its changes.

Categories for which nothing is reported:

Any Product

University of Maine Ice Sheet Model (UMISM)

Dr James L. Fastook

May 13, 2002

Abstract

A multi-component model of ice-sheet physics is presented. Components include mass and momentum conservation for the ice dynamics, energy conservation for the internal temperatures, a hydrostatically supported viscoelastic plate for bed depression and rebound, a conservation of water-based basal water model, and a simple climatology for surface temperatures and mass balance. The model is applied to both paleo- and existing ice sheets. Reconstructions of the Laurentide and Scandinavian Ice Sheets at the LGM are presented, as well as comparisons of the model results with data from Greenland and Antarctica.

Contents

List of Figures

List of Tables

Part I

Introduction

Studies of glaciology as a science began as the earliest researchers recognized that certain geological landforms had been produced by the presence of large sheets of moving ice that had covered wide expanses of the landscape. We have struggled to understand the mechanisms that produced and controlled these ice sheets. Obviously, these moving ice mountains could only have existed if the world were colder. Had they come and gone repeatedly in the past; and if so, how many times? Is it possible that the Ice Age state of the world is actually its normal state? Would the glaciers come again, and when?

Chapter 1

Problems of the Ice Ages

With the advent of radiocarbon dating it became clear that the waxing and waning of the ice sheets had occurred in relatively recent geological time. The existence of these vast moving mountains of ice demonstrated that climate was not constant in time, and that over the last 2.5 million years the ice sheets had come and gone several times, and that, in fact, the world has spent more of its time in a glacial state than it has in the interglacial state of today. With glacial periods typically lasting 100 thousand years, and interglacial periods 10 to 20 thousand years, the Ice Age state is more the norm than the exception.

The imprint of past ice sheets is preserved in various recognizable landforms, such as moraines and till deposits, and the study by glacial geologists of their shape and composition yields clues to the mechanisms of the glaciers that formed them, such as the speed at which the ice advanced and retreated. But present-day topography alone does not offer enough data for us to construct an accurate mechanism of ice sheet behavior. Information on the climate conditions at the time of the Ice Ages must also be added to the picture.

Glacier modelers attempt to combine both topological and climate data to construct a computer-generated "picture," or model, that is able to change over time, just as the ice sheets have. This time dependence is known as dynamic modeling.

1.1 Interpreting cores

The existing ice sheets that remain in Antarctica, Greenland, and other places have preserved some of the best records of past climate available. As one looks deeper into the ice one is looking deeper into the past. Layers of ice near the bottom of present ice sheets may be more than 200 thousand years old, and trace impurities preserved in that ice yield invaluable information about the climate of the world at the time the ice was deposited as snow on the ancient ice sheet.

In the shallow younger ice near the top of the core, actual annual layers in the ice are visibly recognizable and can be relied on to provide an age model for time as a function of depth in the core. Unfortunately as one goes father back in time and deeper into the core, these layers disappear and some other method is necessary to calibrate the time versus depth relationship. This is one of the arenas where dynamic modeling comes into play. In this case, it can be used to show the particle paths of ice as it moves from the surface to depth, by running calculations of assorted Newtonian equations that together comprise a physics-based model of the movement.

Unfortunately the known data by itself is not enough to fill all of the parameters in the motion equations, and so various assumptions are "built into" the model in order to handle the unknowns. Assumptions necessary for such modeling include the past history of the ice sheet (how has it grown or shrunk in the past) as well as its climatic history. In an almost circular argument, one uses the layer-datable upper parts of the core to help define a past chronology that then lets one extract a chronology for the layer-less lower level in the core.

Traditionally, deep cores are drilled at or near the domes of ice sheets, because the dynamics necessary to interpret the depth-time relationship are much simpler there. Domes, usually defined as the highest point on an ice sheet, tend to be located in remote and difficult areas to carry out fieldwork, and deep cores are quite expensive to obtain. As a result, the deep coring of a dome is relatively rare, and when it does occur, requires the full and cooperative resources of several research programs, such as in the US-sponsored Greenland Ice Sheet Program (GISP2) or the European-sponsored Greenland Ice Core Project (GRIP), both of which have successfully drilled cores to the base of the Greenland Ice Sheet.

An alternate form of coring involves the collection of ice along a "horizontal" core where ice is melting at the surface. This ice emerging in a ablation

zone can be very old, having been carried far from its place of deposition. If one is to interpret the trace impurities preserved in this old ice for climatic information, one must again use a dynamic model to calculate the age and place of deposition of the original snow. Horizontal cores, while more difficult to model, are much less expensive and provide a much greater volume of ice for chemical and climatic analysis.

1.2 Reconstructing paleo-ice sheets

Across the landscape various features have been recognized as glacially created or modified. Moraines, eskers, kames, and drumlins are but a few of the geological landforms that are recognized to be glacial in origin. With traditional stratigraphy for relative ages, and radiocarbon for absolute ages, a chronology of ice sheet positions of the past has been developed from study of these landforms across North America, Europe, and Asia. Few of these geological indicators give us any information about the thickness of the ice sheets; instead they only indicate whether ice was or was not present over the landscape at a given time. This is not sufficient for climate modelers trying to model the Ice Age climate. They need to know the shape and elevation of the ice sheets, because one of their primary inputs is the surface topography. To a climate modeler one of the main differences between the Ice Age world and the present is the different distribution of these high albedo ice mountains, which reached elevations of several kilometers and spanned entire continents.

Dynamic models allow us to reconstruct the shape, as well as the outline, of ice sheets of the past. After an outline, or margin of the ice sheet has been identified by glacial geological indicators, the interior thickness can be calculated from various conservation laws and constitutive relationships that make up parts of the model.

As one develops these dynamic models, one necessarily must make some assumptions about various parameters that crop up in the model. These are often constants of proportionality that relate one quantity to another. Often these parameters cannot be determined from first principles, but must be obtained experimentally by laboratory measurement or by comparison of the model output to existing ice sheets. We often calibrate the model (ie., determine the "reasonable" values of the unknown parameters) by "fitting" the output of the model to the known configuration of an existing ice sheet.

1.3 Determining the dynamic state of the existing ice sheets

One problem with the calibration process as mentioned above, is that we often do not know the present configuration of the existing ice sheets all that well. In particular, we do not know if the present configuration is changing with time, or if it is in steady state. Detailed observations of the state of an ice sheet only began a few decades ago, and measuring change on the time scales of the ice sheets is difficult. Field measurements are expensive, time consuming, dangerous, and difficult, and as such we cannot state with great confidence whether the major ice sheets of the world are growing, shrinking, or in steady state. This situation is improving, and with the advent of satellite measurements, data collection is becoming much easier. At the present time, ongoing studies are recording new series of measurements that will better answer these questions.

An important reason for determining the state of the current ice sheets is that the way in which the ice sheets are changing can serve as a climatic indicator. During warm, dry periods we expect the ice sheet margins to retreat. During cool, moist periods we expect them to advance. Ice sheets are tremendous "integrators" of climate: they tend to filter the natural climatic variation and extract out, or smooth, the general trend in the climate. Anyone familiar with the tremendous swings in weather from one year to the next can see how difficult it is to extract a trend from such noisy, short-term data. The ice sheets, with their long response time, filter out the high frequency variations, and respond primarily to the long-term trends.

1.4 Interpreting glacial geology

Glacier modelers depend on glacial geologists to provide them with data constraints on the behavior of their models, while at the same time, the modelers can provide the geologists with a filter for understanding their field data.

For example, geologists often observe gouges or striations on polished outcrops of bedrock. These striations are the primary indicators of the ice flow direction for the field geologist, but often cross-cutting patterns of striations are observed, with two or more sets of marks pointing different directions on the same outcrop. Modelers can help the geologists interpret these data

by providing them with a scenario of ice sheet behavior that will explain the different directions. For example, the models may show that when ice is thin, it is deflected by the topography, whereas when it is thick, it tends to override the topography, hence yielding different flow directions.

1.5 An ice sheet laboratory

In trying to understand the behavior of ice sheets, one cannot design controlled experiments as one does in a laboratory. Numerical models provide the only arena for doing "experiments" on ice sheets. What happens to the shape of an ice sheet as the amount of snowfall increases or decreases? How rapidly does it respond to a change in external conditions? If the climate warms, does the ice sheet get bigger (more snow available from the more moist air) or smaller (more melting by the warmer atmosphere)? How does the warming of the surface due to climatic change penetrate to the bed?

Models can be used to answer these types of"what-if" questions, and they can also act as simulators to allow users to train in the behavior of an ice sheet. As a user controls the model, for example, changing the external temperature, the precipitation patterns, or some interior material property, the result manifests visually as a different or changing ice sheet configuration. How large this change is, or how long it takes for this change to appear, depends on the processes involved and how they are coupled through the physics of the model.

Part II

The Model

Models are theoretical frameworks that allow a more meaningful interpretation of experimental data. The framework must include as complete a description as is possible of the physical processes that produced the experimental data. The description is not formed with words, however, but rather with equations, since of course the data consists of numbers.

Usually the researcher has some intuitive feeling for the processes involved, and this plays a part in the task of converting a complicated physical phenomenon into a series of equations. Comparison of model results with experimental data provides the test as to the correctness of this intuition. When the two are reasonably close, we have some reassurance that the model is a good representation of the physical system.

A good model has predictive capabilities. It can be used to describe the system when it is subjected to a different environment, or to describe the evolution of the system as the controlling conditions change with time.

Importantly, researchers can use the framework to "see" beneath the measurable surface of the system, to make "observations" of quantities that are not experimentally observable.

Chapter 2

Physics-based modeling

There are distinctly different ways to go about constructing the framework of equations in a model and then solving those equations. In all cases one must try to simplify the description of the physical system to a manageable form that will still give accurate results. An ice sheet modeler, for example, must decide which aspects of a landscape can be safely ignored and which ones should be focused on as significant. Deciding what to include and what not to include is one of the most basic assumptions that a modeler makes; other, more complex assumptions are inevitably involved in the process of translating a physical system into a series of equations.

The degree and type of assumptions that are made as a model is being written can be said to form the "character" of the model. Before the computer, physics-based modelers were forced to use restrictive assumptions and simplified domains to allow for an analytic solution of the equations describing their physical system. With the computer, numerical methods can be used to solve the exact equations without such assumptions or simplifications.

The generation and solution of differential equations is fundamental to modeling physical phenomena. How accurate these models are depends on how correct and complete the underlying assumptions are. Both analytic and numerical forms of solutions have their limitations. Numerical solutions require fewer simplifying assumptions, but in the end may provide us with less insight into the importance of various aspects of the model.

Related aspects that also contribute to a model's "character" include the definition of parameters, the initial method of generating the equations (my model starts from the conservation law for mass, momentum, and energy),

and the method chosen to solve the equations.

2.1 Parameters, their use and interpretation

In the formulation of any model, a certain number of parameters must be introduced. These parameters are in some ways a measure of what we don't know about the physics of the model. For instance, in a temperature model, we define the constant that relates the temperature gradient to the rate at which heat flows from a hot to a cold region as the diffusion coefficient. This parameter will then appear in the differential equation we must solve to describe the modeled system. There are theoretical methods whereby one can calculate this parameter from first principles, based on the chemistry of the material, but in practice the diffusion coefficient is usually "measured" by going into a laboratory, and under controlled conditions (ie. removing the possibility of other effects on the rate of heat flow) performing an experiment. The measured diffusion coefficient is that which best "fits" the experimental data.

We have these same kinds of parameters throughout any of our glaciological models. These parameters can be a measure of how resistant the ice is to deformation by an external force, or how easily it moves across its bed. Parameters can be used to relate material properties of the ice to the temperature, or ice densities to pressures and temperatures. Without a way of calculating these parameters from first principles we must obtain reasonable values by calibrating the model. For certain glaciological parameters there is no possibility of a laboratory with controlled conditions and hence we must perform the calibration by comparing to existing ice sheets. In this sense we are "measuring" these parameters by fitting our model results to the experimental data. Of course the validity of these measurements is only as good as our model. Without adequate physics, the measurements will be incorrect, but this is often apparent in our inability to fit the model results to the data.

Chapter 3

Conservation Laws

Conservation laws provide us with one of the most satisfactory methods for generating the equations to use in modeling a physical system. Some fundamental quantity in the system is identified as being conserved, ie. it is neither created nor destroyed within the domain of the problem. Mechanisms are identified that provide sources and sinks of our conserved quantity. Additional mechanisms are identified that allow the fundamental quantity to move about within the domain.

Conservation equations are all based on the consideration of the flux of some physical quantity (such as mass, momentum, or energy) flowing into or out of some region of the domain. This flux is related to a state variable (such as ice thickness, velocity, or temperature) through a constitutive relationship wherein much of the physics of the problem resides. In general the sources and sinks of flux within this region are also considered in arriving at a conservation equation. These fluxes generally depend on position, but they may also depend on the state variable itself, or they may represent fluxes of state variable carried into the region by moving material.

As an example consider a 1-D problem with flux flowing from right to left through some region, and with some distributed sources that are a function of position. We will have a flux in the right-hand side of the region of $\sigma + d\sigma$, balanced by a flux out of the left hand side of $-\sigma$. We will also have a flux due to the distributed source which will be equal to $f(x)dx$, where dx is the width of the differential area. If we are considering a time-dependent problem, the balance of fluxes will also include a term that represents "retention" of flux. This will manifest as a rate of change of the state variable with time, $\frac{\partial u}{\partial t}dx$.

Putting all these pieces together provides the following expression.

$$\frac{\partial \sigma(x)}{\partial x} = f(x) - \frac{\partial u}{\partial t} \tag{3.1}$$

This says that neglecting time-dependent effects, the gradient of the flux at some point in the domain is just equal to the source at that point. An imbalance between these two terms will result in a change in the local state variable, manifest in the time-dependent term. If a portion of the distributed source is proportional to the state variable we may include a term in the right-hand side $b(x)u$. If material moving at a velocity $c(x)$ is carrying flux into the region we may also add a term $c(x)\frac{\partial u}{\partial x}$ to the right-hand side. This term may be considered to originate from the total derivative, $\frac{Du}{Dt}$, given by the chain rule as $\frac{\partial u}{\partial t} + \frac{\partial u}{\partial x}\frac{\partial x}{\partial t}$ where $c(x)$ is $\frac{\partial x}{\partial t}$. In a steady situation $\frac{\partial u}{\partial t}$ is zero, but the "advection" term $c(x)\frac{\partial u}{\partial x}$ will still be present.

Equation (3.1) is not a differential equation, because it is still expressed in terms of the flux, σ, and the state variable, u. To complete the differential equation we need a constitutive relation that relates the flux of the conserved quantity to the gradient of the state variable. A simple example of a constitutive relationship is Fourier's Law, which states that heat, or energy, flows from hot regions to cold regions at a rate which is proportional to the difference in the temperatures between the two regions. Such "Laws" are often based on the experience and intuition of an experimentalist. Fourier's Law for heat flow simply expresses the fact that the flux of heat flowing from a warm region to a cold region is proportional to the temperature gradient between these two regions, where the constant of proportionality is the usual conductivity of the medium. A generic constitutive relation has the form given in the following expression.

$$\sigma(x) = -k(x)\frac{\partial u}{\partial x} \tag{3.2}$$

Combining equations (3.1) and (3.2) we obtain a second-order differential equation.

$$\frac{\partial}{\partial x}\left(-k(x)\frac{\partial u}{\partial x}\right) + c(x)\frac{\partial u}{\partial x} + b(x)u = f(x) - \frac{\partial u}{\partial t} \tag{3.3}$$

For 2- and 3-D domains we will have an analogous equation

$$\nabla \cdot (-k\nabla u) + c\nabla u + bu = f - \frac{\partial u}{\partial t} \tag{3.4}$$

where k, u, c, b and f are functions of position within their respective domains, and the ∇ and $\nabla\cdot$ operators are either 2-dimensional or 3-dimensional gradient and divergence operators.

Thus far we have been dealing with a generic conservation equation. We can apply equation (3.3) or (3.4) to the primary conservation laws of glaciology by making the following identifications. The generic state variable, u, corresponds to the height of the ice surface for the mass conservation equation, to the velocity vector, $\bar{U}$, for the momentum conservation equation, and to the temperature, T, for the energy equation.

Each conservation equation is transformed into a differential equation in terms of its own state variable by the use of a particular constitutive equation corresponding to the generic equation (3.2).

3.1 Mass

For mass conservation this will take the form of the column-averaged flow law which can be expressed for pure flow by the following expression.

$$\sigma = \bar{U}H = -k\nabla h = \frac{2}{n+2}\left[\frac{\rho g|\nabla h|}{A}\right]^n H^{n+2} \tag{3.5}$$

This constitutive relationship relates the flux of mass flowing through the ice column to the surface slope of the ice. This is done by recognizing that the rate at which ice deforms is proportional to the stress (force per unit area) applied to the ice. In the shallow-ice approximation, the only significant stress is the stress acting on the bed (a horizontal surface with the normal in z-direction) in the downstream direction along a flowline (taken for simplicity to be the x-direction). The dominant strain rate is then the gradient of the downstream velocity with respect to depth. The relationship, based on the empirically-derived flow law for ice, is given by the following.

$$\tau = A\left(\frac{1}{2}\frac{du_x}{dz}\right)^{\frac{1}{n}} \tag{3.6}$$

The stress is known to be zero at the top surface, and proportional to the surface slope and the ice thickness at the bed (the so-called "driving stress," $\rho g H|\nabla h|$, which is balanced by the friction at the bed). We integrate this

deformation from the bed to the surface, thereby obtaining the velocity as a function of depth.

$$\int_0^{u_x(z)} du_x = \int_0^z 2\left[\frac{\rho g(h-z)|\nabla h|}{A}\right]^n dz \tag{3.7}$$

$$u_x(z) = \frac{2}{n+1}\left[\frac{\rho g|\nabla h|}{A}\right]^n \left[h^{n+1} - (h-z)^{n+1}\right] \tag{3.8}$$

Since what we are interested in for the differential equation is the flux (average velocity times thickness) we must integrate this depth-dependent velocity again through the thickness to get the average velocity.

$$\bar{U} = \int_0^H u_x(z)\, dz = \frac{2}{n+2}\left[\frac{\rho g|\nabla h|}{A}\right]^n H^{n+1} \tag{3.9}$$

Ultimately we have a relationship between average horizontal velocity in a column and surface slope. Because of the nonlinearity in the relationship between deformation and stress, there will be a nonlinear relation between the flux and the surface slope. This nonlinear problem can be solved by forcing all but a linear term in surface slope into a position-dependent constant, k, which itself depends on the surface gradient, ∇h, and the thickness, H.

$$k = \frac{2}{n+2}\left[\frac{\rho g}{A}\right]^n |\nabla h|^{n-1} H^{n+2} \tag{3.10}$$

This nonlinear problem must then be solved by an iterative process, whereby an initial uniform distribution of k is assumed, a solution for h and H is obtained, a new nonuniform k is obtained from this solution, and the process is repeated until it has converged to a solution. This type of iterative linearized solution is a common technique in dealing with such nonlinear constitutive equations.

3.2 Momentum

The above treatment of the conservation of mass combines explicitly the conservation of momentum through equation (3.6). This approximation, that only the driving stress and companion vertical strain rates are significant, is appropriate for slow-moving inland ice. This approximation may break down for ice streams and regions where other components of stress and strain rates

are significant (the so-called longitudinal stresses, which dominate in shelf flow). To accommodate these terms, the full stress equation with all its components must be solved in the following manner.

For the momentum conservation equation we have a generalized flow law relating stress components to stain-rate components, given by the following expression.

$$\sigma_{ij} = A \left[\dot{\epsilon}^{\frac{n-1}{n}} \right] \dot{\epsilon}_{ij} \tag{3.11}$$

This is just a more generalized version of equation (3.6). used in the mass conservation equation to relate deformation to applied stress. Instead of a single stress component, we now have 9 components of stress (one force in each direction, x, y, and z each applied to the three surfaces normal to each of these directions).

Here $\dot{\epsilon}$ is a strain invariant which depends on all the components of the strain-rate tensor, A is the ice hardness parameter, and the term in the square brackets represents an effective viscosity. Strain rates are related to the gradients of velocity through the following relationship.

$$\dot{\epsilon}_{ij} = \frac{1}{2} \left(\frac{\partial u_i}{\partial x_j} + \frac{\partial u_j}{\partial x_i} \right) \tag{3.12}$$

Again, because of the nonlinear dependence of the flux-like variable σ, on the gradient of the state variable, u, the solution will require a linearization constant, with an iterative procedure to arrive at a self-consistent solution for the velocity vector.

3.3 Energy

Finally, energy conservation uses Fourier's Law relating the heat flux to the temperature gradient given by the following expression.

$$\sigma = -k \nabla T \tag{3.13}$$

where k is the thermal conductivity. Because this conductivity can itself be a function of temperature, this equation must also be solved by an iterative process. We must also allow for the heat that is carried into or out of a region by moving material (the c-term of equation (3.4)) and for internal heat sources generated by the internal deformation of the ice (the f-term of equation (3.4)).

Chapter 4

Solution techniques: Finite Element Method

The finite-element method (FEM) is a standard numerical technique which can be successfully applied to any of these conservation equations, either in a steady-state or a time-dependent situation. The domain on which the conservation equation is to be solved can be complexly irregular, with no need for the curvilinear or normalized coordinates often required by the finite-difference method. Boundary conditions can be easily specified along this irregular boundary as a mixture of essential boundary conditions (specified state variable) or natural boundary conditions (specified flux or specified linear combination of flux and state variable). Gridding within the domain of the problem can be non-uniform and irregular, with the grid spacing adaptable to the smoothness and availability of the underlying data or to the smoothness of the anticipated solution. By appropriate choice of the degree of the interpolating polynomial, derived quantities that depend on derivatives of solved-for quantities can be easily obtained not just at nodal points or element centroids, but at any arbitrary position within the domain of the problem.

4.1 Weak Variational Formulation

Differential equations arising from conservation laws describe the "strong" or classical formulation of the problem. These differential equations must be satisfied at every point within the domain. Solutions for this type of for-

mulation are often impossible because of irregularities and discontinuities in the data describing the problem. For instance, there may be abrupt changes in the various coefficients of equations (3.3) and (3.4) that do not allow for simple solutions. Hence we must look for a "weaker" variational formulation of the problem that will allow for such irregularities in the data.

Consider the steady-state version of the 1-dimensional equation (3.3), and form the residual error function, r, given by the following expression.

$$r(x) = -[k(x)u'(x)]' + c(x)u'(x) + b(x)u(x) - f(x) \tag{4.1}$$

We can multiply this by an arbitrary trial function, v, and integrate over the whole domain, $0 \leq x \leq L$. This can be done only over regions where the data of the problem is smooth. Where the data is insufficiently smooth, we can break the integral into parts spanning smooth regions on either side of the discontinuity. The smooth subdomains are the so-called "elements" of the finite-element method. An integral over one of the subdomains, Ω_i, will be equal to zero, and can be integrated by parts so that the $-[ku']'v$ term becomes symmetric in u and v.

$$\int_{\Omega_i} rv\,dx = -ku'v\Big|_{x_{i-1}}^{x_i} + \int_{\Omega_i} (ku'v' + cu'v + buv)\,dx - \int_{\Omega_i} fv\,dx \tag{4.2}$$

If we have a discontinuity at x_1, a point between 0 and L, we will have from equation (4.2)

$$\begin{aligned}\int_0^L rv\,dx &= \int_0^L (ku'v' + cu'v + buv)\,dx + k(0)u'(0)v(0) + \\ &\qquad \|k(x_1)u'(x_1)\|v(x_1) - k(L)u'(L)v(L) - \int_0^L \bar{f}v\,dx \end{aligned} \tag{4.3}$$

where $\bar{f}$ is the "smooth part" of the source function, f, and the jump condition expressing the discontinuity in $k(x)$ at x_1 is defined by the following.

$$\|k(x_1)u'(x_1)\| = \lim_{x \to x_i^+} k(x)u'(x) - \lim_{x \to x_i^-} k(x)u'(x) = \hat{f}v(x_1) \tag{4.4}$$

Equation (4.3) expresses the ease with which general boundary conditions can be specified in the finite-element method. For the case of essential boundary conditions ($u(0) = u_0$ and $u(L) = u_L$), we simply require that the trial function, v, be precisely zero at the boundaries, and we impose the specified boundary values in the matrix formulation. For natural boundary conditions where the flux is specified at the boundary ($k(0)u'(0) = \sigma(0)$ or $k(L)u'(L) =$

$\sigma(L)$) we simply include these boundary terms explicitly as the second and fourth terms of the right-hand side of equation (4.3). More complex boundary conditions involving linear combinations of the boundary flux and an ambient state variable value can be specified in an analogous manner.

4.2 Galerkin Approximation

Thus far we have succeeded in converting the "strong" formulation of the differential equation into a "weak" symmetric variational formulation. We can now solve this equation by observing that both the solution, $u(x)$, and the trial function, $v(x)$, belong to the same class of functions[1], and hence can be represented by the same infinite sum of basis functions[2]. The essential approximation of the finite-element method involves replacing the infinite series

$$v(x) = \sum_{i=1}^{\infty} \beta_i \phi_i(x) \tag{4.5}$$

with the following finite series.

$$v_N(x) = \sum_{i=1}^{N} \beta_i \phi_i(x) \tag{4.6}$$

We will also have for the unknown solution a similar expression.

$$u_N(x) = \sum_{j=1}^{N} \alpha_j \phi_j(x) \tag{4.7}$$

We can replace u and v in equation (4.3) by their finite summations from equations (4.6) and (4.7). This can be written compactly as the following matrix equation.

$$\sum_{i=1}^{N} \beta_i \left(\sum_{j=1}^{N} K_{ij}\alpha_j - F_i \right) = 0 \tag{4.8}$$

[1] derivatives of order 1 and less are square-integrable over the domain

[2] The Fourier Series is one such infinite-dimensional basis, where $\Psi_n = \sqrt{2}\sin n\pi x$, $v(x) = \sum_{n=1}^{\infty} a_n \Psi_n(x)$ and $a_n = \int_0^1 v(x)\Psi_n(x)\,dx$

Here the matrices K and F, traditionally referred to at the stiffness matrix and load vector, are given by the following expressions.

$$K_{ij} = \int_0^L (k\phi_i'\phi_j' + c\phi_i'\phi_j + b\phi_i\phi_j)\, dx \tag{4.9}$$

$$F_i = \int_0^L \bar{f}\phi_i\, dx + \hat{f}\phi(x_1) - k(0)u'(0)v(0) + k(L)u'(L)v(L) \tag{4.10}$$

We must remember that the trial function, defined by the values of β, is completely arbitrary. Thus we are able to systematically choose values of β and obtain a set of N simultaneous equations in the coefficients, α. This is done by first choosing $\beta(1) = 1$ and all other β's to be zero. This yields the first equation.

$$\sum_{j=1}^{N} K_{1j}\alpha_j = F_1 \tag{4.11}$$

The second equation comes from the choice $\beta_2 = 1$, all other β's zero.

$$\sum_{j=1}^{N} K_{2j}\alpha_j = F_2 \tag{4.12}$$

The process is repeated for all N choices for the β's and the final matrix equation is given by the following.

$$\sum_{j=1}^{N} K_{ij}\alpha_j = F_i, \;\; i = 1, 2, \cdots, N \tag{4.13}$$

4.3 Basis and Shape Functions

Thus far we have made no specifications on the form of the basis functions, ϕ_i which will be associated with the unknown solution coefficient, α_i. It is apparent that once we have specified these basis functions, we can perform the various integrations defining the matrices in equation (4.13), and solve the matrix equation for the unknown coefficients, α, from which the shape of the solution can be constructed using equation (4.7). We do require that they be square-integrable over the domain. We will impose one further condition that will make the identification of the α's more transparent. If we specify that each basis function be equal to one at precisely one element boundary

or node, and precisely zero at all other nodes, then the solution for the α's yields us precisely the solution for the u's at each of these nodes. With the condition

$$\phi_i(x_j) = \begin{cases} 1 & \text{if } i = j \\ 0 & \text{if } i \neq j \end{cases} \tag{4.14}$$

equation (4.7) becomes

$$u_N(x) = \sum_{j=1}^{N} u_j \phi_j(x) \tag{4.15}$$

where u_i replaces α_i and can be identified as the value of the solution at the node x_i.

We can build such basis functions in a piece-wise manner over the smooth subdomains or elements by combining element shape functions which are only defined within a particular element. For example, in Figure 4.1 we show a 7-node, 6-element 1-dimensional domain. Also shown by the solid line on the figure is the basis function ϕ_4, corresponding to the fourth node. Note that this basis function is precisely 1 at node 4, and precisely zero at all others. It is apparent that this basis function satisfies the requirements of being square-integrable over the domain, and that it has the required differentiability; i.e., that first derivatives exist.

Focusing on the region of the basis function where it is nonzero (from node 3 to node 5), we see that it is composed of two pieces, one that is zero at node 3 and 1 at node 4 (element 3) and one that is 1 at node 4 and zero at node 5 (element 4). These two pieces represent individual shape functions from these two elements. Also note that each element contains pieces that will contribute to precisely two basis functions. We define the shape functions, Ψ, on a particular element to have the properties that Ψ_i is precisely one at the i^{th} node of the element, and that it is precisely zero at all the other nodes in the element. Thus basis function ϕ_4 is composed of shape function Ψ_2 from element 3 and shape function Ψ_1 from element 4. By the same reasoning we could assemble in a piece-wise manner basis functions for each of the nodes in the domain from precisely two of the shape functions from the two adjacent elements.

Now we look back at the integrals from 0 to L of equations (4.9) and (4.10) that were used to define the various entries in the stiffness matrix and the load vector. First we notice that integrals of a single basis function, or of

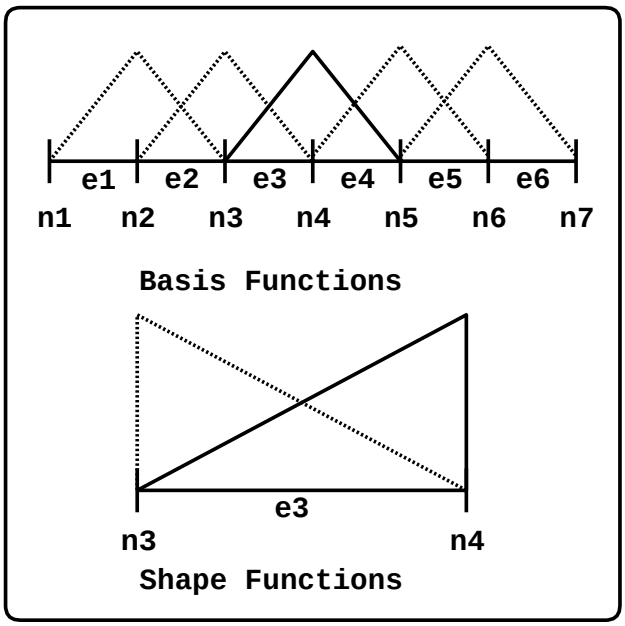

Figure 4.1: Basis and shape functions

a basis function times itself, need only be integrated over the nonzero region of the basis function. Thus K_{44} and F_4 only need only be integrated from node 3 to node 5 as opposed to over the entire domain. Terms involving dissimilar basis functions, such as K_{34} or K_{43}, need only be integrated over the region where the two basis functions overlap, namely element 3. If we break up our global integration from 0 to L into separate integrations over each element, we find that there are only four contributions to the global stiffness matrix, and that there are only two contributions to the global load vector. Thus for each element we will have expressions analogous to equations (4.9) and (4.10). These are the element stiffness matrix and load vector, and the indices i and j range from 1 to the number of nodes in an element, N_e.

$$k_{ij}^e = \int_{x_e}^{x_{e+1}} \left(k_e \Psi_i' \Psi_j' + c_e \Psi_i' \Psi_j + b_e \Psi_i \Psi_j\right) dx \tag{4.16}$$

$$f_i^e = \int_{x_e}^{x_{e+1}} \bar{f}_e \Psi_i \, dx \tag{4.17}$$

Performing the global integration of the N basis functions over the entire domain collapses to performing local integration of the N_e shape functions over the individual elements and judiciously combining these element matrix entries together to form the global matrices. Traditionally one defines the shape functions in terms of local element coordinates. Integration is then performed in terms of these local coordinates and the results scaled by the Jacobian of the transformation to the global coordinate system. This allows the automation of the matrix formation to be performed quite efficiently for irregular and complex arrangement of the elements.

4.4 Extension to 2- and 3-Dimensions

Modification for extension to higher dimensionality is quite straightforward. All derivatives with respect to x become ∇ operators, and the integration by parts is replaced by the following vector identity.

$$\nabla \cdot (k \nabla u v) = \nabla \cdot (k \nabla u) v + k \nabla u \cdot \nabla v \tag{4.18}$$

The integration with respect to x is replaced with integration with respect to area for the 2-D case, and with respect to volume for the 3-D case. The boundary terms originating from the integration by parts can be transformed with Green's formula into a line integral along the boundary for the 2-D case, and into a surface integral for the 3-D case.

4.5 Time-dependent Solution

Throughout the previous discussion we have neglected the presence of the time-dependent term $\frac{\partial u}{\partial t}$ in equation (3.3). If we are to solve a time-dependent problem it is necessary to include this term in the residual formed in equation (4.1). This will give rise to an additional term in the matrix equation, traditionally called the capacitance matrix, C_{ij}.

$$\sum_{j=1}^{N} C_{ij} \frac{\partial u_j(t)}{\partial t} + \sum_{j=1}^{N} K_{ij} u_j(t) = F_i(t), \quad i = 1, 2, \cdots, N \tag{4.19}$$

Here C_{ij} is given by

$$C_{ij} = \int_0^L (\phi_i \phi_j)\, dx \tag{4.20}$$

We can develop an implicit, numerically stable, backward-difference scheme by using the following approximation, where n indicates the time step.

$$\frac{\partial u^n}{\partial t} = \frac{u^n - u^{n-1}}{\Delta t} \tag{4.21}$$

Substituting equation (4.21) into (4.19) and suppressing subscripts and summation we obtain an expression relating the solution at one time step to the solution at an ensuing time step.

$$\left(\frac{C}{\Delta t} + K\right) u^n = F^n + \frac{C u^{n-1}}{\Delta t} \tag{4.22}$$

Interestingly this form of the equation is identical to the form of the steady state solution where the stiffness and load vectors are modified by the capacitance matrix.

Part III

Model Components

The application of these models to the ice sheet problem is complex and inter-related [7]. In the descriptions of the mass and momentum conservation equations we see a parameter appearing that is a measure of the ice hardness. This quantity is known to depend strongly on the temperature. Hence to accurately model mass conservation, which gives us the shape of the ice sheet, or momentum conservation, which give us the velocities within the ice sheet, we must know the temperature field within the ice sheet. But recall that the energy conservation model, from which we obtained this temperature field, itself required both the ice sheet shape as well as the internal velocity field. Indeed, the momentum conservation model itself requires the shape and the mass conservation model requires some internal approximation of the velocities. Each of the individual conservation models requires some input from each of the other models. For a complete description of the ice sheet we must solve each of the conservation laws, mass for the ice sheet shape, momentum for the internal velocities, and energy for the internal temperatures.

Chapter 5

ice dynamics

5.1 The Continuity Equation

A discussion of the equations governing the flow of ice must begin with an evaluation of the conservation of mass. Mass conservation requires that the net flux into a region be balanced by changes in the ice thickness of that region. There are three factors involved in the mass balance of an ice sheet: 1) the rate of accumulation or ablation; 2) the change in ice surface elevation with respect to time; 3) the divergence of ice flux density.

Balancing fluxes into and out of a differential area with the rate of thickening in that area yields a continuity equation of the form

$$\nabla \cdot \sigma(x, y) = \dot{a}(x, y) - \frac{\partial h}{\partial t} \tag{5.1}$$

The accumulation rate, $\dot{a}$, represents the net total of both the snow fall rate and the melting rate at a point (x, y) of the domain.

To complete this equation one must relate the flux, σ, to the ice surface elevation, h, through a constitutive equation. For non-Newtonian fluids such as ice, this involves a nonlinear relationship depending on the ice surface elevation, the thickness, and the surface slope. We can, however, linearize this by absorbing all dependencies on h and all nonlinearities in the surface slope into a spatially nonuniform proportionality constant, $k(x, y)$. This constitutive equation relating ice flux to surface slope can be expressed by

$$\sigma(x, y) = -k(x, y)\nabla h(x, y) = UH \tag{5.2}$$

The material coefficient $k(x, y)$ is dependent upon several material properties of ice. The physical basis for this relationship and the nature of the dependency of $k(x, y)$ on the material properties of ice will be made clear with further evaluation of the ice velocity, U. The bed topography relates ice thickness, H, to ice surface elevation, h.

In glacier flow the ice behaves like a stack of pages, each page above moving relative to the one below it, with the bottom-most page affixed to the bed. The strain rate (change in length per unit length per unit time) is related to the driving stress by a non-linear flow law of the form [5, 16, 24]

$$\frac{1}{2}\frac{\partial u}{\partial z} = \dot{\epsilon} = \left[\frac{S}{A}\right]^n \tag{5.3}$$

where the $\frac{1}{2}$ derives from this being a shear deformation. Neglecting longitudinal stresses, S at the bottom of the ice column is simply the basal traction, given by $\tau = \rho g|\nabla h|H$ [17]. Since the stress must be zero at the free top surface of the ice column, a simple expression for S as a function of depth is

$$S(z) = \rho g|\nabla h|(H - z) \tag{5.4}$$

where the coordinate system is such that z is zero at the bed and H at the surface. Integrating equation (5.3) from the bed where velocity is equal to the sliding velocity (if sliding is occurring) to some depth z one obtains the velocity as a function of depth [10].

$$u(z) = U_S + \frac{2}{n+1}\left[\frac{\rho g|\nabla h|}{A}\right]^n \left[(H - z)^{n+1} - H^{n+1}\right] \tag{5.5}$$

Integrating equation (5.5) from the bed to the surface and dividing by the thickness yields the column-averaged ice velocity necessary for the flux calculation of the FEM.

$$U = U_S + \frac{2}{n+2}\left[\frac{\rho g|\nabla h|}{A}\right]^n H^{n+1} \tag{5.6}$$

Later in 6.2 the ice hardness parameter, A is shown to depend strongly on the ice temperature, and this explicit integration will be replaced with a numerical integration that takes into account the variation of temperature within the ice column. The ice hardness parameter that appears in equation (5.6) can be taken to represent an effective ice hardness, i.e., that which will pass exactly the same flux as the numerically-integrated ice column.

Under certain conditions ice can slide over its bed. This process is not well understood, but evidence indicates that ice can move as a block with a nonzero velocity at the bed and with little or no internal shear. Sliding appears to depend on the concentration of debris in the ice at the ice-bed interface, the ice grain size, the presence of air bubbles in the ice, the permeability of the bed, the degree to which the the bed can be deformed, the amount of water at the ice-bed interface, the roughness of the bed, the subglacial water pressure, and cavitation [17].

The sliding law used here is a general relationship for beds at the melting point developed by Weertman [21, 22]. It depicts movement over a rough bed which occurs as a result of melting on the high-pressure upstream side of an obstacle followed by subsequent refreezing on the low-pressure downstream side. The sliding law constant, B, and the sliding law exponent, m, can be used to absorb the effects of the various conditions influencing sliding. Weertman's theory yields the following expression for a sliding velocity that is uniform with depth.

$$U_S = \left[\frac{\rho g|\nabla h|}{B}\right]^m H^m \tag{5.7}$$

We modify this slightly to incorporate the effect of the water layer at the base of the ice, which is expected to represent the mechanism that produces sliding.

$$U_S = C_S \left[\rho g|\nabla h|\right]^p H^p w^q \tag{5.8}$$

where C_S incorporates the Weertman Sliding Constant, B, $\rho g H \nabla h$ is the driving stress, and p and q are exponents to be chosen.

The form of $k(x, y)$ is obtained by combining equations (5.6), (5.8), and (5.6) and substituting into equation (5.2).

$$k(x,y) = -\left(\left[\frac{\rho g}{B}\right]^m H^{m+1}|\nabla h|^{m-1} w^q + \left[\frac{2}{n+2}\right]\left[\frac{\rho g}{A}\right]^n H^{n+2}|\nabla h|^{n-1}\right) \tag{5.9}$$

This shows the dependence of the material coefficient on ice density, gravity, flow law constant and sliding law constant (both of which are dependent on ice temperature, ice crystal size, impurity content, etc.), ice thickness, surface gradient, and water thickness.

Substituting the constitutive law expression for $\sigma(x, y)$ from equation (5.2) into continuity equation (5.1), yields the following differential equation in h.

$$\nabla \cdot (-k(x, y)\nabla h) = \dot{a}(x, y) - \frac{\partial h}{\partial t} \tag{5.10}$$

The presence of $k(x, y)$ in the continuity equation incorporates the physics of the flow and sliding laws into the problem, since its form depends on the form of the flow and sliding law. Different treatments of the flow and sliding process change the form of $k(x, y)$ but do not affect the method with which the problem is solved. An entirely different sliding relationship can be substituted without materially affecting the ensuing discussion leading to a solution to this equation.

With the continuity equation determined, all that remains for a complete description of the problem is a discussion of boundary conditions. The FEM allows for both essential and natural boundary conditions. Natural boundary conditions encompass situations where the flux is specified along a portion of the boundary, while essential boundary conditions require the specification of the ice height along a portion of the boundary.

Chapter 6

Thermodynamics

6.1 Internal Temperatures

Internal temperatures are determined by solving the vertical, z, 1-D heat-flow equation (6.1)

$$\frac{\partial T}{\partial t} = \kappa \frac{\partial^2 T}{\partial z^2} - w \frac{\partial T}{\partial z} + \frac{Q}{\rho_i c} \tag{6.1}$$

where κ is the thermal diffusivity, $\rho_i c$ is the ice density, and c is the specific heat. The left-hand side expresses the temperature changing with time. On the right-hand side, the first term describes the diffusion of heat, the second term expresses the advection of heat by ice moving in the vertical direction with velocity w, and the third term expresses internal heat generated within the column.

Since this is a 1-D equation solved for each nodal point in the 2-D map-plane ice sheet model, both horizontal diffusion and advection are neglected. This is reasonable in the case of diffusion, but for fast flowing ice streams horizontal advection (the introduction of heat carried in by moving material) may become important. Since most lakes are near ice divides or are well in the interior, we do not need to deal with this here.

The primary source of internal heat is shear between layers in the vertical, which dominates for flow, and basal friction, which dominates for sliding.

Boundary conditions consist of a specified surface temperature (from measurements or from climatic parameterizations) and a basal temperature gradient (related to the geothermal heat flux).

In solving equation (6.1) one must account for the possibility that the solution can yield temperatures which exceed the pressure melting point (PMP) within the column. In this case, one must change the form of the boundary condition from a specified gradient to a specified temperature at the PMP and re-solve the equation. With this new boundary condition, the basal temperature gradient is different from that specified by the geothermal heat flux. The difference is provided by the latent heat of fusion released by ice melting. It is this melt water that contributes to the basal hydrological system which will be discussed in (8.

An additional possibility that must be accounted for is that the calculated temperature at the bed drops below the PMP although there is water present. Again, the basal boundary condition must be reset to a basal temperature specified at the PMP and the equation re-solved. Again, the difference between the calculated gradient and the geothermal gradient is accommodated by the latent heat of fusion, produced in this case by freezing of water onto the base of the ice column.

The end result of the temperature calculation gives the temperature of the bed, which is less than or equal to the PMP, and provides an estimate of the rate of melting or freezing that is occurring at the bed.

6.2 Flow law constant, dependence on temperature

Beginning with Paterson 1981 [17] we find

$$\dot{\epsilon}_{XZ} = A\tau_{XZ}^{n} \tag{6.2}$$

where

$$A = A_0 \exp(-Q/RT) \tag{6.3}$$

where $R = 8.314$ J/mol-^{o}K is the gas constant, and Q for temperatures less than -10 ^{o}C is in the range 42-84 KJ/mole, with a usable value of 60 KJ/mole [24]. For temperatures greater than -10 ^{o}C, Q appears to depend on temperature, but a value of 139 KJ/mole is given [15]. This temperature-dependent value of the ice hardness parameter must be used in the numerical integration of the strain rates in equation (5.5) through the vertical that is key to the evaluation of equation (5.6) in 5.1.

Chapter 7

Isostacy

7.1 Introduction to the deforming bed

Full treatments of the Earth's crust, mantle, and core for glacial modeling are often computationally overwhelming, in the sense that the time requirements to calculate a full self-gravitating spherical Earth model for the time-varying load history of an ice sheet, are considerably greater than the time requirements for the ice dynamics and thermodynamics combined. For this reason, we adopt a "reasonable" approximation for the behavior of the deforming bedrock beneath the ice sheet and solve it with an efficient C^0 Finite Element Method (FEM) [12].

Geophysicist have used the observed rebound of the Earth's crust following ice sheet collapse and consequent unloading of the crust to probe the interior of the Earth. Early estimates of crust and mantle properties came from analysis of the rate, magnitude, and spatial distribution of uplift at the presumed centers of major ice sheets in the context of a simple hydrostatically supported elastic crust with specified thickness and mechanical properties[9].

Other modelers [18, 19, 20] used the measured relative sea levels, a consequence of depression and rebound, around known ice sheets, coupled with a detailed theoretical model of the Earth's interior to place constraining limits on possible ice thicknesses, both spatially and temporally, at the domes of these ice sheets.

The Earth models used by the latter group, the self-gravitating spherical Earth models, usually require modeling the entire Earth through the use of Green's Functions or Laplace Transforms, which must be numerically inte-

grated over both space and time. The time integration usually requires a priori knowledge of the loading history (the ice sheet thicknesses as a function of time) in order to make predictions of local relative sea levels, which can then be compared with field data. By adjusting the load histories, a "best fit" Earth response is obtained, which then constrains the possible ice thicknesses that could have existed over the duration of the hypothetical ice sheets.

Ice sheet modelers are faced with a different problem. They are trying to model the behavior of the ice sheet as it responds to both external forcings such as changing climate or sea level, as well as internal dynamics, such as a possible surge-like behavior produced by internal temperature oscillations at the bed [11, 14]. As such, their models require the calculation of the bedrock response to a load history that is only known up to the instant of one individual integration forward in time. Often internal feedback mechanisms controlling the ice dynamics depend directly on degree of depression of the bedrock itself, so it is not possible to calculate the ice sheet load history and the bedrock depression history independently.

Ice sheet modelers often use simplified Earth models to approximate the behavior of the underlying bedrock. One such simplification is the hydrostatically supported elastic plate mentioned above. We will show how this can be solved efficiently using the FEM, as well as how it can be extended to the more realistic viscous Newtonian and even non-Newtonian fluid cases.

This simple model of the Earth treats the crust as an elastic plate supported from below by a hydrostatic fluid. Conservation of linear and angular momentum for an elastic plate leads to the classical Poisson-Kirchhoff fourth order differential equation in the crustal displacement, w, given by the following equation

$$EI\nabla^4 w = L(x,y) - \rho g w \tag{7.1}$$

where EI are material properties that depend on the crust's elastic properties and its thickness, $L(x,y)$ is the load produced by the ice column at a point, ρ is the crust's density, and g is the acceleration of gravity. This equation is easily solved when restricted to one dimension with a C^1 FEM [3]. Such a method requires basis function continuity both at the function and derivative level, and is traditionally done with piecewise-constructed Hermite Polynomials for basis functions.

C^1 FEMs are difficult to implement in more than one dimension, and as such the engineering community has turned away from classical Poisson-

Kirchhoff plate theory to treatments such as Reissner-Mindlin plate theory, which are able to accommodate transverse shear and hence require only C^0 continuity of basis functions (only the function, and not the derivative, is required to be continuous at the element boundary) [12]. This method reduces the complexity of the C_1 formulation by adding additional degrees of freedom (the transverse shear in x and y) at each node.

7.2 Reissner-Mindlin Plate Theory

7.2.1 RMPT Assumptions

In formulating the Reissner-Mindlin plate theory, we will make a number of basic assumptions, the most fundamental of which is that the 3-dimensional x, y, z domain can be approximated by a 2-dimensional x, y domain where all properties are defined at the middle of the plate of thickness t ($-t/2$ to $+t/2$) that itself can be a function of x and y.

A second fundamental assumption is the plane stress hypothesis, which basically states that the stress in the z-direction, acting on a surface with normal in the z-direction is zero.

$$\sigma_{33} = 0 \tag{7.2}$$

This assumption allows us to solve for and ultimately eliminate ϵ_{33} from the constitutive relationship[1]

The final two assumptions deal with the representation of the x, y, and z strains, $u_i(x, y, z)$. We take the x and y components to be representable in terms of a rotation angle, θ, which itself is not a function of z. A physical interpretation of this assumption is that the angle θ represents the rotation of a fiber that is initially normal to the plate midsurface ($z = 0$).

$$u_\alpha(x, y, z) = -z\theta_\alpha(x, y) \tag{7.3}$$

At the same time, we represent the z component of the strain, u_3, as a transverse displacement, w, which is also not a function of z.

$$u_3(x, y, z) = w(x, y) \tag{7.4}$$

[1]In the notation used here, Latin indices take on the values 1, 2, and 3, representing x, y, and z, whereas Greek indices take on the values 1 and 2, representing x and y, respectively. A repeated index, such as ϵ_{kk} in equation (7.5), implies summation over the full range of the index, so $\epsilon_{kk} = \epsilon_{11} + \epsilon_{22} + \epsilon_{33}$.

An astute observer might point out that this last assumption contradicts the plane stress hypothesis. However, because it works well in engineering applications, and it greatly reduces the complexity of the formulation (indeed, few plate theories are fully consistent with 3-dimensional theory), we will use it here.

7.2.2 Constitutive Relation

Conservation Laws in general do not yield a differential equation until some assumptions are made about the behavior of the material in question. This usually manifests as a hypothetical constitutive relationship, which in our case will relate stresses and strains. The simplest case is a linear isotropic material (Hooke's Law), given by the following.

$$\sigma_{ij} = \lambda \delta_{ij} \epsilon_{kk} + 2\mu \epsilon_{ij} \tag{7.5}$$

Here λ and μ are the Lamé coefficients and δ_{ij} is the Kronecker delta.

It is worth noting at this point that this constitutive relationship for an elastic material is identical in form to the constitutive relationship for a viscous material, except that the strains, ϵ, in the elastic form are replaced by strain rates, $\dot{\epsilon}$, in the viscous form (and of course the Lamé coefficients take on a different meaning, μ, for instance becomes the viscosity). The unknown displacements solved for in the elastic case are thus replaced by rates of displacement in the viscous case, and displacements can be obtained from some type of time-step differencing scheme. Almost all subsequent discussion of how to solve this plate problem is thus applicable to either the elastic or the viscous case.

The plane stress hypothesis ($\sigma_{33} = 0$) allows us to solve for ϵ_{33} in equation (7.5) above.

$$\epsilon_{33} = \frac{-\lambda}{\lambda + 2\mu} \epsilon_{\alpha\alpha} \tag{7.6}$$

This allows us to then write the planar form of equation (7.5) as the following two equations, one (7.7) for surfaces with normals in x and y, and the other (7.8) for surfaces with normals in z.

$$\sigma_{\alpha\beta} = \bar{\lambda} \delta_{\alpha\beta} \epsilon_{\gamma\gamma} + 2\mu \epsilon_{\alpha\beta} \tag{7.7}$$

$$\sigma_{\alpha 3} = 2\mu \epsilon_{\alpha 3} \tag{7.8}$$

In equation (7.7) above, we have introduced $\bar{\lambda}$, given by the following, to simplify the equations and preserve the original form of the 3-dimensional equation (7.5).

$$\bar{\lambda} = \frac{2\lambda\mu}{\lambda + 2\mu} \tag{7.9}$$

Finally, we can express the strains (or strain rates, in the viscous case) in terms of the displacements (or rates) by the following[2].

$$\epsilon_{\alpha\beta} = u_{(\alpha,\beta)} = -z\theta_{(\alpha,\beta)} \tag{7.10}$$

$$\epsilon_{\alpha 3} = u_{(\alpha,3)} = \frac{-\theta_\alpha + w_{,\alpha}}{2} \tag{7.11}$$

7.2.3 Definitions

Table 7.1 indicates the notation that will be used in the subsequent discussion of the FEM solution of the Reissner-Mindlin Plate Theory.

7.2.4 Variational Equation

The traditional method for developing the equations of motion for any physical system using a variational calculus approach involves writing down an expression that forms the product of a virtual displacement times the forces (internal energy), balanced against all of the external forces doing work on the body (also expressed with virtual displacements). In our case this involves strains times stresses (or later as we will see, strain rates times stresses) and applied body forces and external tractions and torques. The internal energy terms look like the following.

$$\int_\Omega \epsilon_{ij}\sigma_{ij}\, d\Omega = \int_\Omega u_{(i,j)}\sigma_{i,j}\, d\Omega \tag{7.12}$$

Breaking it into (x, y) planar and z vertical terms and including the plane stress condition ($\sigma_{33} = 0$)

$$\int_\Omega \epsilon_{ij}\sigma_{ij}\, d\Omega = \int_A \int_{-t/2}^{+t/2} \left[u_{(\alpha,\beta)}\sigma_{\alpha,\beta} + 2u_{(\alpha,3)}\sigma_{\alpha,3}\right] dz\, dA \tag{7.13}$$

[2]The notation $u_{(\alpha,\beta)}$ is defined to represent the symmetric part of the displacement gradients, $(u_{\alpha,\beta} + u_{\beta,\alpha})/2$. Here also the comma between indices implies differentiation with respect the coordinate corresponding to a particular index. For instance, $w_{,\alpha}$ means $\partial w/\partial x$ and $\partial w/\partial y$.

w	:	transverse displacement
θ_α	:	rotation vector
$m_{\alpha\beta} = \int_{-t/2}^{+t/2} \sigma_{\alpha\beta} z \, dz$	:	moment tensor
$q_\alpha = \int_{-t/2}^{+t/2} \sigma_{\alpha 3} \, dz$	:	shear force vector
W	:	prescribed boundary displacement
Θ_α	:	prescribed boundary rotations
$F = \int_{-t/2}^{+t/2} f_3 \, dz + < h_3 >$	:	applied force per unit area
$C_\alpha = \int_{-t/2}^{+t/2} f_\alpha z \, dz + < h_\alpha z >$	:	applied couple per unit area
$M_\alpha = \int_{-t/2}^{+t/2} h_\alpha z \, dz$	:	prescribed boundary moments
$Q = \int_{-t/2}^{+t/2} h_3 \, dz$	:	prescribed boundary shear force
$< f(x,y,z) >= f(x,y,-t/2) + f(x,y,+t/2)$	:	definition

Table 7.1: Definitions used

Expressing this in terms of the definitions above we obtain the following.

$$\int_\Omega \epsilon_{ij}\sigma_{ij}\, d\Omega = \int_A (-\theta_{(\alpha,\beta)} m_{\alpha\beta} + (-\theta_\alpha + w_{,\alpha}) q_\alpha)\, dA \tag{7.14}$$

Externally originated terms include forces and torques applied to the body, as well as on the surface.

$$-\int_A (-\theta_\alpha C_\alpha + wF)\, dA - \int_{S_k} (-\theta_\alpha M_\alpha + wQ)\, ds \tag{7.15}$$

Combining equations (7.14) and (7.15), which must add to zero, we have an expression of the conservation of both linear and angular momentum.

$$\begin{aligned} 0 \;=\; & \int_A (-\theta_{(\alpha,\beta)} m_{\alpha\beta} + (-\theta_\alpha + w_{,\alpha}) q_\alpha)\, dA \\ & - \int_A (-\theta_\alpha C_\alpha + wF)\, dA \\ & - \int_{S_k} (-\theta_\alpha M_\alpha + wQ)\, ds \end{aligned} \tag{7.16}$$

Integrating by parts, with appropriate boundary terms appearing we have the following.

$$\begin{aligned} 0 \;=\; & \int_A \theta_\alpha (m_{\alpha\beta,\beta} - q_\alpha + C_\alpha)\, dA \\ & - \int_A w(q_{\alpha,\alpha} + F)\, dA \\ & - \int_{S_k} \theta_\alpha (-m_{\alpha n} + M_\alpha)\, ds \\ & - \int_{S_k} w(q_n - Q)\, ds \end{aligned} \tag{7.17}$$

It is easy to see that the first term above expresses moment equilibrium, the second term transverse equilibrium, while the third and forth terms express applied moment and shear boundary conditions[3]. Expressed as the strong form (satisfied at a point) we have a moment equation

$$m_{\alpha\beta,\beta} - q_\alpha + C_\alpha = 0 \tag{7.18}$$

and a transverse equation

$$q_{\alpha,\alpha} + F = 0 \tag{7.19}$$

[3]For surface with normal n_α, $m_{\alpha n} = m_{\alpha\beta} n_\beta$ and $q_n = q_\alpha n_\alpha$

Recalling the definition of the moment tensor as the following,

$$m_{\alpha\beta} = \int_{-t/2}^{+t/2} \sigma_{\alpha\beta} z \, dz \tag{7.20}$$

and substituting the planar constitutive equation (7.7) plus equations (7.9) and (7.10) and integrating with respect to z, we obtain the following.

$$m_{\alpha\beta} = -\frac{t^3}{12}(\bar{\lambda}\delta_{\alpha\beta}\theta_{\gamma,\gamma} + 2\mu\theta_{(\alpha,\beta)}) \tag{7.21}$$

Similarly for the shear force vector

$$q_\alpha = \int_{-t/2}^{+t/2} \sigma_{\alpha 3} \, dz \tag{7.22}$$

we substitute the transverse constitutive equation (7.8) plus equation (7.11) and integrate with respect to z and obtain the following.

$$q_\alpha = t\mu(-\theta_\alpha + w_{,\alpha}) \tag{7.23}$$

Note here that if we limit ourselves to one dimension ($\alpha = \beta = x$), solve equation (7.18) for q_α and substitute into equation (7.19), apply no moments ($C_\alpha = 0$), and require zero shear strain ($\theta_x = w_{,x}$, classical Poisson-Kirchhoff beam theory) we obtain the following differential equation in w, the vertical displacement, which is exactly analogous to equation (7.1) where the hydrostatic support term is included in the external transverse load term, F.

$$\frac{t^3}{12}(\bar{\lambda} + 2\mu)w_{,xxxx} = F \tag{7.24}$$

Equations (7.18), (7.19), (7.21), and (7.23) can be further combined, expressed as integrals over the domain of the problem with appropriate weighting functions for the various degrees of freedom (the weak form), and converted to the symmetric form by a vector/matrix identity with useful boundary terms arising from the application of Gauss's Theorem[4]

[4]This is beyond the scope of this paper, but a detailed description of this procedure can be found in Chapter 5 of *The Finite Element Method: Linear Static and Dynamic Finite Element Analysis* by T.J.R. Hughes [12].

Chapter 8

Basal Water

8.1 Flux Model

A flux relationship, like those discussed at length in [3], is used to model the movement of water under ice. The variable under consideration in this model is w, the depth, or thickness of liquid water under the ice. The term thickness may be confusing. It is used because the water is above the till and below the ice, thus the thickness of a layer.

The flux equation, from continuity, is

$$\frac{\partial w}{\partial t} = -\vec{\nabla} \cdot \vec{\sigma} + \dot{S}. \tag{8.1}$$

where $\vec{\sigma} = \vec{V} w$,$\vec{V}$ is the velocity vector, and $\frac{\partial w}{\partial t} = \dot{w}$ is the time rate of change of water thickness.

The $\dot{S}$ term represents external sources or sinks of water. Specifically, $\dot{S}$ is the rate of melting or re-freezing taking place at the bottom of the ice sheet. This amount is calculated from the heat generated by the temperature module of the ice sheet model that is discussed in (6.1).

8.2 The Water Velocity

Equation (8.1) is the continuity equation describing flow in a basal water system. Before the model can be put to use, the flux quantity $\vec{\sigma}$ must be determined. This is done by specifying the velocity.

An appropriate choice of velocity is the Manning equation. This equation relates the velocity to the potential gradient. The equation is stated here and developed from first principles in the following discussions.

$$V = \frac{1}{n} R^p \left[\frac{\nabla \Phi}{\rho_i g} \right]^q \tag{8.2}$$

The equation includes a parameter, n, the roughness coefficient, as well as the hydraulic radius, R, defined as the cross sectional area of the wetted region divided by its perimeter. The exponents p and q vary according to whether the flow is laminar or turbulent.

Specification of the parameters in equation (8.2) is important. In a finite element scheme with square elements with side l the hydraulic radius is $\frac{w2l}{4l} = \frac{w}{2}$.

This value of the hydraulic radius amounts to treating an entire grid element of a finite element mesh as a rectangular conduit. In this way, the relation between the small scale features of channelized basal water flow and the much courser features of a typical finite element grid is made. Such a treatment is not entirely out of the ordinary. [2] uses the same approach, and modelers of open channel phenomena such as flood plains have successfully applied Manning's equation.

The values of the exponents are $p = 2$, $q = 1$ for laminar and $p = \frac{1}{2}$, $q = \frac{2}{3}$ for turbulent flow. To determine if the flow is laminar or turbulent, the Reynold's number is computed with

$$R = \frac{\rho_w V w}{2\mu}. \tag{8.3}$$

Here, μ has been introduced as the viscosity of water.

The roughness coefficient varies over about a factor of three for turbulent flow, depending on the substance the water is flowing through([23]).

Finally the velocity is clearly a vector quantity. To make direction perfectly clear the following form of equation (8.2) is used.

$$\vec{V} = \frac{1}{n} \left(\frac{w}{2} \right)^p \left(\frac{1}{\rho_i g} \right)^q |\nabla \Phi|^{q-1} \vec{\nabla} \Phi \tag{8.4}$$

8.3 The Pressure Potential

The previous section demonstrated that the velocity is dependent on a potential gradient. The exact form of this potential is determined here.

The pressure potential of the basal water system must account for both the topography of the bed and the load of ice. The desired expression results from summing the ice overburden pressure and the effective head (with respect to sea level). An additional term N, is included to account for differences between the ice overburden pressure and the actual water pressure. N is called the effective pressure and is thought of as the portion of ice load supported by the bed.

The ice overburden pressure is expressed by $\rho_i g H$, where ρ_i is the density of ice, g is acceleration due to gravity, and H is the thickness of the ice. The effective head with respect to sea level can be written as $\rho_w g z_b$, with ρ_w the density of water, and z_b the elevation of the bed. The effective pressure, N, is calculated with the relation given by [1]

$$N = k_n \frac{\tau}{f}. \tag{8.5}$$

With constant k_n, and f, the fraction of the bed that is submerged in some specified area. f is a simple parameterization generally taken as a function of w, that relates to the geometry of the bed. Taking $f = w$ for the rest of the discussion, any differences due to bed geometry can be accommodated in k_n.

The resulting expression for the pressure is

$$\Phi = \rho_i g H + \rho_w g z_b - N. \tag{8.6}$$

Equation (8.6) is simplified by noting that the ice thickness, H, can be written as the difference between surface elevation, z_s and bed elevation z_b. Furthermore, driving stress is written

$$\tau = \rho_i g (z_s - z_b) |\nabla z_s| \tag{8.7}$$

giving the new expression for the potential

$$\Phi = \rho_i g z_s - \rho_i g \left(\frac{\rho_w}{\rho_i} - 1 \right) z_b - k_n \frac{\rho_i g (z_s - z_b) |\nabla z_s|}{w}. \tag{8.8}$$

Or, by using known values for the densities and simplifying

$$\Phi = \rho_i g \left(z_s - 0.09 z_b - k_n \frac{(z_s - z_b) |\nabla z_s|}{w} \right). \tag{8.9}$$

8.3.1 A Differential Equation for Water Thickness

The basic flux relationship can now be rewritten in a manner that is specific to the water problem. Starting with equation (8.1),

$$\dot{w} = -\vec{\nabla} \cdot \left(w\vec{V} \right) + \dot{S}. \tag{8.10}$$

Substituting equation (8.4) into equation (8.10) yields a differential equation in terms of water thickness and pressure gradients.

$$\dot{w} = -\vec{\nabla} \cdot \left(k(w, |\nabla\Phi|)\vec{\nabla}\Phi \right) + \dot{S}. \tag{8.11}$$

where the non-linear constant, k, which depends on both the water thickness, w, and the potential pressure, Φ has the following form.

$$k(w, |\nabla\Phi|) = \frac{w^{p+1}|\nabla\Phi|^{q-1}}{n2^p(\rho_i g)^q} \tag{8.12}$$

Equation (8.11) is a first-order non-linear differential equation in terms of w, solving it will yield the thickness of water under the ice sheet at a specified time.

8.3.2 FEM for First-order Non-linear Equation

The finite element method is used to solve this in the following way by eliminating derivatives of the non-linear constant and converting the problem to a matrix equation.

The Galerkin Method, with trial function v is applied to equation (8.11).

$$\int_\Omega \dot{w}v \, d\Omega = -\int_\Omega \nabla \cdot (k\nabla w)v \, d\Omega + \int_\Omega \dot{S}v \, d\Omega \tag{8.13}$$

The vector identity for forming the symmetric formulation is

$$\nabla \cdot (k\nabla wv) = \nabla \cdot (k\nabla w)v + k\nabla w \cdot \nabla v \tag{8.14}$$

Equation (8.13) becomes

$$\int_\Omega \dot{w}v \, d\Omega = \int_\Omega k\nabla w \cdot \nabla v \, d\Omega - \int_\Omega \nabla \cdot (k\nabla wv) \, d\Omega + \int_\Omega \dot{S}v \, d\Omega \tag{8.15}$$

The second term on the right-hand side of (8.15) can be converted to a boundary integral by Stoke's Theorem, and with appropriate boundary conditions, ignored.

$$\int_\Omega \nabla \cdot (k\nabla wv) \, d\Omega = \int_{\delta\Omega} k\nabla wv \, d\delta\Omega \tag{8.16}$$

Equation (8.15) then becomes just

$$\int_\Omega \dot{w} v \, d\Omega = \int_\Omega k \nabla w \cdot \nabla v \, d\Omega + \int_\Omega \dot{S} v \, d\Omega \tag{8.17}$$

The usual FEM approximation, in terms of basis functions, ψ is

$$w_h = \sum_{j=1}^{N} w_j \psi_j \tag{8.18}$$

$$\Phi_h = \sum_{j=1}^{N} \Phi_j \psi_j \tag{8.19}$$

and the trial function, v is

$$v_h = \psi_i \;\; (i = 1, N) \tag{8.20}$$

Substituting equations (8.18),(8.19), and (8.20) into (8.17)

$$\begin{aligned} \sum_{j=1}^{N} \left[\int_\Omega \psi_i \psi_j \, d\Omega \right] \dot{w}_j \;\; = & \\ & \sum_{j=1}^{N} \left[\int_\Omega \left(k \frac{\partial \psi_i}{\partial x} \frac{\partial \psi_j}{\partial x} + \frac{\partial \psi_i}{\partial y} \frac{\partial \psi_j}{\partial y} \right) d\Omega \right] \Phi_j \\ & + \int_\Omega S \psi_i \, d\Omega \end{aligned} \tag{8.21}$$

The bracketed terms are matrices (capacitance and stiffness) and the last term is a vector (load)

$$M_{ij} = \int_\Omega \psi_i \psi_j \, d\Omega \tag{8.22}$$

$$K_{ij} = \int_\Omega \left(k \frac{\partial \psi_i}{\partial x} \frac{\partial \psi_j}{\partial x} + \frac{\partial \psi_i}{\partial y} \frac{\partial \psi_j}{\partial y} \right) d\Omega \tag{8.23}$$

$$F_i = \int_\Omega S \psi_i \, d\Omega \tag{8.24}$$

Equation (8.21) becomes (with summation now implied)

$$M_{ij} \dot{w}_j = K_{ij} \Phi_j + F_i \tag{8.25}$$

which can be solved

$$w^{t+\Delta t} = w^t + \Delta t M^{-1}(K\Phi + F) \tag{8.26}$$

Note here that the capacitance matrix, M, depends only on the geometry, so only needs to be formed once and inverted to obtain M^{-1}. The stiffness matrix, K, will need to be formed for each time step, since it depends on w and $\nabla\Phi$. The right-hand side of equation(8.26) itself requires no inversion, since the vector multiplied by the stiffness matrix, K, is the potential vector, Φ, rather than the unknown, w. Thus the right-hand side is evaluated by matrix multiplication. If the capacitance matrix can be lumped into a diagonal matrix, the inverse is trivial, $(\Delta t/d_{ii})$, and can be dotted with the vector $(K\Phi + F)$.

Chapter 9

Climatology

9.1 Mass Balance Parameterization with Lapse Rates

The primary input, besides the bedrock topography, is the mass balance at each node. In modeling existing ice sheets measured values of accumulation rates can be used. However, if experiments dealing with changing climate are desired, some self-consistent mass-balance relationship that accounts for changes in the ice configuration is necessary. In the ideal we would couple such an ice sheet model with a global circulation model (GCM), so that changing topography and albedo would be able to affect the ice sheet's own climatic conditions. With GCMs too expensive and complicated, a simpler parameterization of the ice sheet's affect on local climate is required for efficient experimentation. We developed a mass-balance relationship based on empirically fitting to present Antarctic accumulation rates. This relationship depends on surface elevation, surface slope, and latitude. Complementary ablation rates are based on South Greenland mass-balance data, and are appropriate for modest warming of the Antarctic climate. The climate is adjusted by varying the mean annual sea-level air temperature, T_{NSL}, which provides a starting point for all temperature calculations at present sea level. We understand the limitations of this very simplified model of the mass balance, but feel that it is an appropriate approximation to the actual situation.

The mass-balance relationship follows Fortuin and Oerlemans [8] with modifications suggested by Jourzel and Merlivat [13] and Braithwaite and Olesen [4].

Basically this involves a surface temperature derived from a lapse rate and modified for distance from the pole.

$$T_S = A_L * h + B_L * L_{AT} + C + T_{NSL} + 14.0 \tag{9.1}$$

This surface temperature can also be used for the top-surface boundary condition in the temperature solution when actual climatic data is not available, or when climate-change scenarios are being run.

From this surface temperature, a free atmosphere-isothermal layer temperature is obtained.

$$T_F = 0.67 * (T_S + 273.0) + 88.9 \tag{9.2}$$

This temperature is used to calculate the saturation vapor pressure from a standard meteorological relationship.

$$T_{ERM1} = -9.09718 * (273.16/T_F - 1.0) \tag{9.3}$$

$$T_{ERM2} = -3.56654 * LOG(273.16/T_F) \tag{9.4}$$

$$T_{ERM3} = 0.876793 * (1.0 - T_F/273.16) + 0.785835 \tag{9.5}$$

$$E_X = T_{ERM1} + T_{ERM2} + T_{ERM3} \tag{9.6}$$

$$E_S = 10^{E_X} \tag{9.7}$$

Finally the accumulation rate is obtained from a fit of accumulation versus saturation vapor pressure and surface slope.

$$A_{CC} = W * E_S + X * S_{LOPE} + Z - 15.276 * S_{HAPE} \tag{9.8}$$

Ablation is modeled by calculating the number of positive degree days based on assumptions of the seasonality as a function of latitude. We calculate a seasonality factor

$$Q_Y = \frac{1}{12} \sum_{I=1}^{12} QI_I - QS_I * L_{AT} \tag{9.9}$$

and a monthly mean temperature

$$T_I = T_S + 0.021 * ((QI_I - QS_I * L_{AT}) - Q_Y) \tag{9.10}$$

and then sum up the positive degree days

$$P_{DD} = \sum_{I=1}^{12} 30. * T_I \tag{9.11}$$

from which we calculate the ablation rate.

$$A_{BL} = .6 * P_{DD} \tag{9.12}$$

Finally, the net mass balance is the difference between these two.

$$\dot{a} = A_{CC} - A_{BL} \tag{9.13}$$

Fortuin and Oerlemans [8] estimated parameters for the various fitting equations from available Antarctic data. We have used the Scott Polar map as digitized by Budd [6]. This data provides surface elevation, ice thickness, bedrock elevation, surface temperature, accumulation rate, and balance velocity for a 20 km grid centered on the South Pole (241X241 grid).

The following are the values obtained for the monthly seasonality factors. For QI_I we use 960, 1036, 1200, 825, 330, 90, 150, 600, 1200, 1020, 930, and 850. For QS_I we use 0.667, 4.6, 11.667, 9.167, 3.667, 1.0, 1.667, 6.667, 12.0, 6.333, 0.333, and -3.333. Other fitting parameters obtained include $A_L = -9.62376690$, $B = -0.546917617$, $C = 24.9793854$, $W = 19.1390686$, $X = 0.922791243$, and $Z = -0.738900483$.

9.2 Mass Balance Parameterization from Current Climate DATA

This new mass-balance scheme uses time series of gridded weather data to derive an annual net mass balance usable in an ice sheet model such as UMISM. It is based on the NCEP Reanalysis data provided by the NOAA-CIRES Climate Diagnostics Center, Boulder, Colorado, USA, from their Web site at http://www.cdc.noaa.gov/. The NCEP data set spans the time period from 1/1/1948 to the present, with spatial coverage of 1.875-degree latitude x 1.875-degree longitude on a global grid with 192x96 points. The principles of extracting net mass balance would be the same for any gridded set, whether it be actual data or results from a GCM.

The NCEP data set contains *monthly means* for 2 m temperatures at 1.875 degree spacing for the Earth for the years 1948 to the present. The

data set also contains monthly means for the net precipitation. We also include a 1.875-degree topography map extracted from the ETOPO5 data set of bathymetry and topography. From these three data sets we will extract net annual mass balance (accumulation of frozen precipitation minus ablation due to melting).

The monthly means for each of temperature and precipitation are give for each of the months in the 22 year period spanned by the data. We average these to obtain a mean monthly mean for both temperature and precipitation. Thus 12 monthly values for temperature and precipitation are available for each of 192X96 points spaced 1.875 degrees apart for the whole globe.

The first step involves generating a *mean annual temperature* for each point. This involves a straight-forward summing and averaging of the 24 values (2 years times 12 months). Since we are interested in being able to produce temperature for a landscape that is itself changing as the ice sheets thicken and thin, we include a lapse-rate based decline in this mean annual temperature depending how far above the base topography the particular point's elevation is. This lapse rate, typically between -3 and -9 degrees/km is an *adjustable parameter* in the scheme. In addition, there is a *global climate parameter*, used to vary the whole climate of the Earth. This is added to (for warmer) or subtracted from (for colder) this mean annual temperature.

The mean annual temperature is important for the UMISM, since this is a fundamental boundary condition in the internal ice temperature solution, from which ice material properties, basal melting rates, and the component of sliding are derived. Previous mass balance schemes were based exclusively on this mean annual temperature, a situation we mean to improve with this new scheme.

To calculate the net mass balance, we need an estimate of two components, the accumulation rate (positive) and the ablation rate (negative).

The ablation rate we obtain from a Positive Degree Day (PDD) calculation. Potential for melting has been shown to depend strongly on the number of PDDs (PDDs are the sum of the number of degrees above freezing). This is easily obtained from the monthly mean temperatures. For each month, the number of PDDs is just the monthly mean minus 273.16 times the number of days in the month. With the two-year data set, the final sum of PDDs must be divided by two. Potential for melting is given by some constant times the number of PDDs. This constant, typically 0.003 to 0.006 m/PDD, is an *adjustable parameter* in the scheme. Note that the global climate parameter has already been added to the monthly means used in this calculation, so

that a colder climate would have fewer PDDs for a particular location.

The accumulation rate is a bit more complicated, since the data set only contains monthly mean precipitation amounts, and it is not segregated into solid and liquid form. As such we divide the total precipitation for a month into either snow (mean annual temperature for the month is below freezing) or rain (mean annual temperature for the month is above freezing).

In using the global climate parameter to warm or cool the climate, we must also recognize that warming or cooling the climate will also affect the amount of precipitation available for partitioning into snow or rain. We expect that cooling will decrease available precipitation, whereas warming will lead to an increase. As such we utilize the following parameterization (obtained from, and also used in the EISMINT Greenland experiment).

For a climate warmed by ΔT, increase available precipitation by a multiplicative factor F where

$$F = 1.05^{\Delta T} \tag{9.14}$$

For a cooling $\Delta T < 10^o$, the factor is

$$F = (1.05 - 0.005\Delta T)^{\Delta T} \tag{9.15}$$

And for cooling $\Delta T > 10^o$, the factor is

$$F = 1.1^{\Delta T} \tag{9.16}$$

At this point we have the accumulation rate (the amount of precipitation partitioned into snow per year) and the ablation rate (proportional to the number of PDDs). We also have the mean annual temperature. All of these can depend on the elevation of the point, relative to the baseline topography (temperature declines with a lapse rate) as well as the global climate parameter, which serves to shift all temperatures by the same amount. Adjustable parameters then include

- global climate parameter
- conversion between PDDs and melt rate
- lapse rate with elevation
- factor offsetting temperature at which precipitation is partitioned into either snow or rain

As was mentioned, there is a "climate knob" that can be used to cool or warm the whole Earth. doing so will change all the mean temperatures by the same amount, and hence change the number of PDDs as well as the partitioning of precipitation into snow and rain. This will of course alter the distribution of net mass balance. With the temperature knob at zero (the present), we obtain the a particular partition into snow and rain. This will change as the climate knob is changed, hence altering the accumulation rate and the net mass balance.

Bibliography

[1] R.B. Alley. Water-pressure coupling of sliding and bed deformation: I. Water system. *Journal of Glaciology*, 35(119):108–118, 1989.

[2] R.B. Alley. Towards a hydrological model for computerized ice-sheet simulations. *Hydrological Processes*, 10(4):649–660, 1996.

[3] E.B. Becker, G.F. Carey, and J.T. Oden. *Finite Elements, An Introduction*. Prentice-Hall, Englewood Cliffs, 1981.

[4] R. J. Braithwaite and O. B. Olesen. Calculation of glacier ablation from air temperature, West Greenland. In J. Oerlemans, editor, *Glacier Fluctuations and Climate Change*, pages 219–233. Kluwer Academic Press, Dordrecht, 1989.

[5] W.F. Budd. The dynamics of ice masses. Technical Report 108, National Antarctic Research Expedition, Australia, 1969.

[6] D.J. Drewry. Antarctica: Glaciological and geophysical folio. Technical report, Scott Polar Research Institute, University of Cambridge, Cambridge, England, 1983.

[7] J.L. Fastook. A map-plane finite-element program for ice sheet reconstruction. In Keith R. Billingley, Hilton U. Brown, and Ed Derohanes, editors, *Computer Assisted Analysis and Modeling on the IBM 3090, Volume 1*, pages 45–80. The Baldwin Press, The University of Georgia, Athens, Georgia, 1992.

[8] I.P.F. Fortuin and J. Oerlemans. Parameterization of the annual surface temperature and mass balance of Antarctica. *Annals of Glaciology*, 14:78–84, 1990.

[9] G.D. Garland. *Introduction to Geophysics: Mantle, Core, and Crust.* W.B. Saunders Company, Philadelphia, Londan, Toronto, 2nd edition, 1979.

[10] J.W. Glen. The creep of polycrystalline ice. *Proceedings of the Royal Society of London*, 228:519–538, 1955.

[11] R. Greve and D.R. MacAyeal. Dynamic/thermodynamic simulations of Laurentide ice-sheet instability. *Annals of Glaciology*, 23:328–335, 1996.

[12] Thomas J.R. Hughes. *The Finite Element Method: Linear Static and Dynamic Finite Element Analysis.* Prentice-Hall, Inc., Englewood Cliffs, New Jersey, 1987.

[13] J. Jouzel and L. Merlivat. Deuterium and oxygen 18 in precipitation: Modeling of the isotopic effects during snow formation. *Journal of Geophysical Research*, 89:11749–11757, 1984.

[14] D.R. MacAyeal. Binge/purge ocsillations of the Laurentide Ice Sheet as a cause of the North Atlantic's Heinrich events. *Paleoceanography*, 8:775–784, 1993.

[15] Mellor and Testa. Effect of temperature on the creep of ice. *Journal of Glaciology*, 8:131–145, 1969.

[16] J.W. Nye. The motion of ice sheets and glaciers. *Journal of Glaciology*, 3:493–507, 1959.

[17] W.S.B Paterson. *The Physics of Glaciers.* Pergamon, Oxford, 2nd edition, 1981.

[18] W.R. Peltier. Ice age paleotopography. *Sciences*, 265:195–201, 1994.

[19] A.M. Tushingham and W. R. Peltier. ICE-3G: A new global model of Late Pleistocene deglaciation based upon geophysical predictions of post-glacial relative sea level change. *Journal of Geophysical Research*, 96:4497–4523, 1991.

[20] A.M. Tushingham and W. R. Peltier. Validation of the ICE-3G model of Wurm-Wisconsin deglaciation using a global data base of relative sea level histories. *Journal of Geophysical Research*, 97:3285, 1992.

[21] J. Weertman. On the sliding of glaciers. *Journal of Glaciology*, 3(21):33–38, 1957.

[22] J. Weertman. The theory of glacier sliding. *Journal of Glaciology*, 5, 1964.

[23] J. Weertman. General theory of water flow at the base of a glacier or ice sheet. *Reviews of Geophysics and Space Physics*, 10, 1972.

[24] J. Weertman. Creep of ice. In E. Whalley, S.J. Jones, and L.W. Gold, editors, *Physics and Chemistry of Ice*. Royal Society of Canada, Ottawa, 1973.

A Basal Water Model for Ice Sheets

By

Jesse V. Johnson

B.S. University of Minnesota, Twin Cities

A THESIS

Submitted in Partial Fulfillment of the

Requirements for the Degree of

Doctor of Philosophy

(in Physics)

The Graduate School

The University of Maine

April, 2002

Advisory Committee:

James L. Fastook, Professor of Computer Science, Advisor

Terence J. Hughes, Professor of Geological Sciences

Susan McKay, Professor of Physics

Neil Comins, Professor of Physics

Kirk Maasch, Associate Professor of Geological Sciences

External Reader:

Christina Hulbe, Assistant Professor of Geology, Portland State University

A Basal Water Model for Ice Sheets

By Jesse V. Johnson

Thesis Advisor: Dr. James L. Fastook

An Abstract of the Thesis Presented
in Partial Fulfillment of the Requirements for the
Doctor of Philosophy
(in Physics)
April, 2002

An previously existing ice sheet model is described. The model accounts for ice deformation, themo-mechanical coupling, isostasy, and simple climatology. After reviewing the current and past literature pertaining to the melt water systems that exist within glaciers and ice sheets, a basal water model for ice sheets is formulated. The model takes the form of a conservation equation for basal water coupled with a relationship for the velocity of basal water and an expression for the potential field experienced by the basal water system. The model also accounts for basal water flowing through a permeable under-layer based on some assumptions about the till that is under ice sheets. The differential equations that arise from formulation of the model are solved numerically with the finite element method. The model is tested for its sensitivity to various physical parameters. A sliding law is formulated in terms of the basal water distribution. The first set of tests is conducted on the Ross Ice Streams of Antarctica. The parameters considered are the interaction with the aquifer and the velocity of the water. The study demonstrates that with a proper sliding law,

an accurate reproduction of the positions and the velocities of the Ross Ice Streams is possible. The second sensitivity test considers the glaciation and de-glaciation of the Northern Hemisphere. The second test demonstrates a clear advantage of ice sheet models that use a basal water distribution to estimate sliding over models that simply have sliding whereever the bed is thawed. With a basal water model for ice sheets, it is possible to identify sub-glacial lakes from topological data sets. This is done in Antarctica. The position of the sub-glacial lakes identified from data sets compares favorably with the position of sub-glacial lakes identified in field studies. The set of sub-glacial lakes are analyzed for their stability and potential contribution to a basal water system. It is shown that sub-glacial lakes can play a significant role in maintaining or stagnating ice streams.

CHAPTER 3

HYDROLOGICAL MODEL FOR ICE SHEETS

3.1 Introduction

The focus of this thesis is the development of a numerical model for the flow of liquid water beneath ice sheets. This chapter presents an overview of previous work on glacial water systems. The discussion then moves to how the existing body of work, much of it of a theoretical and idealized nature, be applied in a numerical model. Finally, a set of relations to represent the flow of water beneath ice sheets is presented. Subsequent chapters address the success of the modeling scheme and demonstrate applications of the work.

A basal water model is useful for a number of reasons. Glacial melt water is an important source of water in many regions where the promise of summer rains is unreliable. Several European nations have utilized melt water for hydroelectric power generation. In Iceland, periodic outbursts of meltwater from beneath glaciers flood large areas, destroy civic works, and sometimes kill people. The flooding is so regular and well documented it has been given the name jökulhlaup: a sudden and rapid drainage of a glacier dammed lake or of water impounded in a glacier (Paterson (1994a)). Jökulhlaups have also been observed in Antarctica, Norway, Switzerland, Canada, Alaska, New Zealand, Pakistan, and South America. Estimates of the area flooded by such events are as much as 100 km^2.

On a much larger scale, outbursts of glacial melt water explain of the "channeled scab lands" of Eastern Washington state, which cover an area of 5000 km^2. In this case it seems that the water was on the surface of the ice, rather than beneath it. Brennand et al. (1994); Shaw (1996); Shaw et al. (1996) all report catastrophic

outbursts that shape landscapes. If such geomorphological features are indeed the result of outbursts of glacial melt water, they are consistent with modeling results from very large ice sheets. Contrast such flooding to the jökulhlaup events in Iceland and elsewhere which correspond to water stored in relatively small glaciers. These mega-floods, as they have been called, are a compelling reason for modeling studies, as the volumes of fresh water released in such events could be sufficient to alter local and perhaps even global climate patterns (Grosswald, 1999).

Finally, and perhaps most importantly, the study of basal water is worthwhile because basal water is at the very heart of glacial sliding. Sliding ice accounts for fully 90 percent of the ice being shed from western Antarctica. It moves between 10 and 100 times more quickly than ice that is moving due to internal deformation, called creep. In the extreme case of a surge, the velocities of the sliding ice can exceed 1000 times that of ice that is only creeping.

There are a range of theories for sliding; several of them are discussed in Section 2.4. In reviewing sliding theories it is clear that the most significant factor is the condition of the bed of the ice sheet (Paterson, 1994a). This condition is most easily characterized by distinguishing between frozen and thawed beds. More complex sliding theories are expressed in terms of the volume or pressure of the sub-glacial water system. If such schemes are to be used, it is important that the distribution of water beneath an ice sheet be well characterized. A comparison of sliding schemes and their impact on a glaciation cycle is the topic of Chapter 5. Sliding velocities, and how they compare to field data are discussed in Chapter 4.

3.2 Theories on Glacial Water Flow

There is a substantial body of work related to the flow of water through glaciers. Much of it is theoretical and applied to idealized situations such as a perfectly circular tunnel, or water flowing over a sinusoidally varying bed. There is also a small body

of experimental evidence on the way that water flows through glaciers: the velocities, the volumes, etc. The existing work is often applied to features much smaller than the current resolution of ice sheet models. That is to say, the approaches consider formations that span tens of meters, whereas the ice sheet model uses a 5 km or greater spacing of points at which the solution is computed. In spite of the very different spacial scales in modeled and theoretical schemes, there are many concepts in the literature that prove useful in developing a basal water model. The nature and scope of the work is reviewed here. Subsequent sections will detail how this body of work can be applied.

3.2.1 Englacial Flow

Much of the work in glacial hydrology involves the study of temperate glaciers. These are glaciers that are near the melting point everywhere except at the surface, where seasonal temperature changes can be measured. The hydrology of these glaciers is important, as they are a source of fresh water for some communities, a source of hydroelectric power for others, and a source of floods for still others. Temperate glaciers have also been studied because these glaciers are more accessible than the ice sheets found in remote regions of the world, and the characteristics of their flow can be tested with dye tracer experiments that begin on the surface of the glacier.

Temperate glaciers are characterized by surface melting in the summer. This meltwater then enters the interior of the glacier through a network of crevasses and veins (small, triangular tubes in temperate ice, measuring about 25 μm across) in the ice (Raymond and Harrison (1975)). Once in the glacier, the water forms moulins, or tunnels in the ice, that can extend all the way to the base of the ice sheet and the terminus of the glacier. The direction of water flow through the glacier is idealized as normal to equipotential surfaces in the glacier. The moulins have a tendency to close due to the creep of ice, but are also held open due to viscous heating from the water

traveling through them. These two competing tendencies can be used to determine the dimensions of the moulin.

Shreeve (1972) provides the classic analysis of englacial flow that is the starting point for many other authors. Englacial flow provides much of the theoretical framework for basal flow. The important concepts from Shreeve's work include the following:

- The *water pressure potential* is defined in general terms as

$$\phi = \phi_0 + p + \rho_w g z. \tag{3.1}$$

  Here ϕ_0 is a reference potential, p is the water pressure, and z is the height above some reference point, generally sea level, ρ_w is the density of water and g is the acceleration due to gravity. Water flows down the potential gradient. This pressure potential accounts for the pressure within the water system as well as the height of the terrain relative to sea level. A relation between p and the ice overburden pressure is developed in subsequent sections.

- The velocity of the water within a moulin can be estimated by the Manning equation. This equation is also used to estimate the velocity of water in the basal water model, and discussed in Section 3.4.3.

- The amount of heat available to melt the walls of a moulin is proportional to the change in potential energy of the water as it moves down slope minus the amount of energy required to keep the water from freezing. This concept is key to the computation of pressure in englacial tunnels.

- There are two competing tendencies in glacial water flow. There is a tendency for conduits to close, due to the deformation of ice. There is also a tendency for the conduits to remain open, due to the viscous heating of the conduit walls. This is the basis for many of the theoretical models to come.

Other important aspects of englacial flow have been characterized by Röthlisberger (1972). He found a non-linear differential equation in p by equating the rate of tunnel closure due to the deformation of ice and the rate a tunnel melting due to water running through it. The closing of a tunnel from the creep of ice is described by Nye (1953). The details of the derivation of the differential equation is a standard for text book writers and appears in Paterson (1994a) and Hooke (1998). For clarity the equation is stated here as

$$\left[\rho_w g \sin\theta + \frac{dp}{ds}\right]^{\frac{11}{8}} - E\left(\frac{dp}{ds}\right)\left[\rho_w g \sin\theta + \frac{dp}{ds}\right]^{\frac{3}{8}} = K_1 L \rho_i (\rho_w g)^{\frac{3}{8}} n'^{\frac{3}{4}} A (P-p)^3 Q^{-\frac{1}{4}}. \tag{3.2}$$

θ is the angle of the passage with respect to horizontal, s is the co-ordinate in the direction of flow, E and K_1 are dimensionless constants, L is the latent heat of fusion, n' is the Manning roughness coefficient, A is the flow law parameter from Equation 2.30, P is the ice overburden pressure, and Q is the water flux.

The equation is important because it is the first analytic expression to relate the water pressure, p, to the water flux, Q. Curiously, Equation 3.2 shows that the water pressure increases for decreased flow, although the dependence is not strong ($Q^{-\frac{1}{4}}$). This has a very important consequence. Supposing that two tunnels come into contact, the tunnel having the a greater flux will be favored, as the higher pressure in the smaller flux tunnel forces flow into the larger flux tunnel. This idea is consistent with the observed formation of arborescent drainage networks.

Equation 3.2 can be integrated numerically and used in a flow line model of a temperate glacier. It can also be simplified by considering the relative order of magnitude of each term (Fowler (1987)). One problem with such an approach is that the flow law parameter, A and Manning roughness, n' are very uncertain.

3.2.2 Basal Water Flow

Basal water flow, or sub-glacial flow, is distinguished from englacial water flow by its interaction with the underlying bed. I have divided the discussion into two key parts. The first deals with the flow of water between a glacier and an impermeable bed consisting of bedrock. The second part deals with the flow of water between the ice and an underlying glacial till that is permeable. The two are referred to as hard and soft bed respectively.

3.2.2.1 The Hard Bed

Some efforts to understand basal water flow focus on the analytic expression in Equation 3.2. Basic agreement of the equation and field data is not good. Pressures measured in the field tend to be much higher than Equation 3.2 would predict. Two important issues that need to be addressed are that the derivation of 3.2 involved a circular tunnel and that it assumed stresses were normal to the tunnel walls. Neither of these assumptions apply to basal water flow. Field studies show that the tunnels emerging from a glacier's terminus resemble low arches. Furthermore, there are important stresses that are parallel to the orientation of the tunnel.

Accounting for these important differences between englacial and basal water flow, Hooke et al. (1990) was able to obtain good agreement between theory and field data by introducing an angle to describe the tunnel as a small section of a large circle. Hooke then repeated the derivation of Equation 3.2 with the new geometry and applied the new equation to the well known Storglaciären of Sweden. While this method accurately reproduced field data, it uses an estimate of a quantity that is generally unknown (the angle describing the tunnel) to get a quantity that is known (the pressure). The angles used were reasonable, but there is not currently a method to check them.

Other analyses of basal or sub-glacial water flow have focused on the idea of an

intricate network of cavities, interconnected by orifices. The idea here is that there are bumps in the bed, the ice flows over the bumps and leaves an opening on the lee side of the bumps opposite ice flow. Figure 3.1 illustrates this. When conditions are right, there is melting at the bed, and the cavity on the lee side of the bump fills with melt water. The cavities are linked by much smaller features, called orifices. Investigation of a recently deglaciated bed reveals that there are indeed small channels incised in the rock that correspond to the orifices between cavities (Walder and Hallet (1979)). There are also regions near the steps or bumps that could be cavities, as they lack the normal abrasions exhibited by bedrock that has been overridden by glacial ice. The dimensions of such a system are a function of the bedrock topography. Analysis by Kamb (1987) indicates that the important dimensions for such a system are cavities approximately 1 m high and 10 m long, and orifices of 10 cm or less.

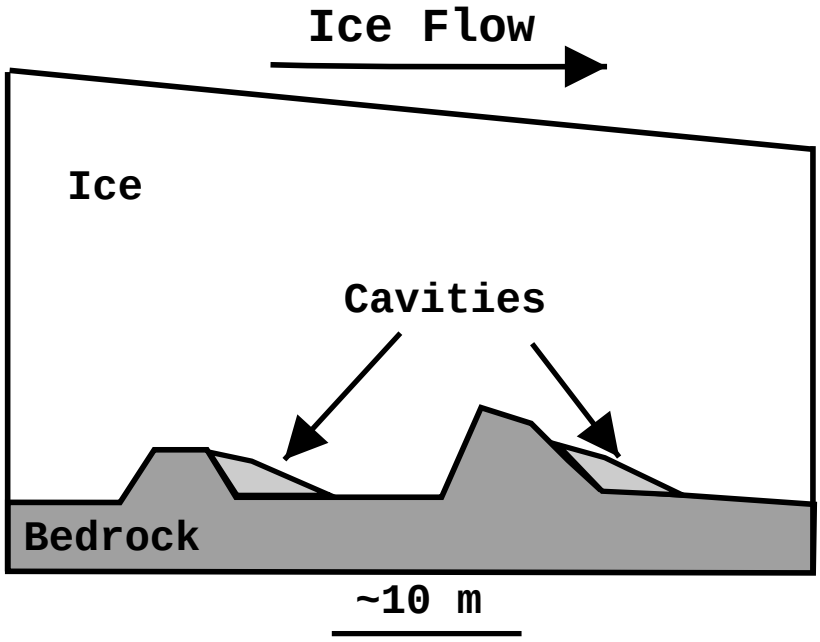

Figure 3.1: A side view of bedrock and ice showing the positions of cavities on the lee side of bumps.

The orifice and cavity idea was originated by Lliboutry (1968). Steady flow of

water in such a system was first analyzed by Walder (1986). Walder assumes that the cavities are held open by the ice sliding overhead (in addition to the viscous heating), that the bed is horizontal, and that the initial pressure gradient is uniform. The size of the cavity is computed from ice dynamics, and the sliding velocity. A flux of water through the system is computed with the Manning equation.

The work of Walder (1986) results in the interesting conclusion that the water flux increases with increasing pressure. This is contrary to the conclusions of Röthlisberger (1972) detailed in the previous section, which showed an inverse relation between pressure and water flux. A direct relation between flux and pressure means that a system of linked cavities is stable, and will not change to an arborescent drainage system.

Kamb (1987) applied the linked cavity system to explain surge behavior. According to Kamb, surges take place when there is an abrupt change from a linked cavity system to a tunnel system. Because orifices control the flow between cavities, they are considered in detail. In particular the relationship between the shape of the roof of the orifice and the velocity of the ice above the orifice is considered. The change from linked cavities to tunnels is determined by something called the "orifice stability parameter". This parameter characterizes the tendency for an orifice to stay open due to the viscous heating provided by the water, as well as the tendency for orifices to close due to the gravitational creep of ice. Some simplifying assumptions are made due to the irregular geometry of the orifices. Namely, it is assumed that the rheology of ice is linear with an appropriate viscosity, and that there is no advection of heat. The resulting orifice stability parameter is

$$\Xi = \frac{2^{1/3} S^{1/2}}{\sqrt{\pi} \Lambda n'} \left(\frac{\mu}{u_b P_c} \right) h^{7/6} \tag{3.3}$$

where Λ is a constant involving the latent heat of fusion, μ is the equivalent Newtonian viscosity (found from a linearization of Equation 2.1) of ice, u_b the sliding speed, h is the thickness of the ice over the orifice, and S is the hydraulic head corrected for the

sinuosity of flow.

Ξ dictates the shape of the orifice. According to the analysis, as Ξ increases, the roof of the orifice becomes more arched. As Ξ approaches a value of 1.0, the orifice becomes unstable because the orifice's dimension in the direction of ice flow increases without bound. This instability may explain the transformation from a linked cavity system to a system of tunnels.

Finally, in Weertman (1972) and Weertman (1986) compelling arguments for water moving in a sheet beneath the ice are made. The argument accounts for large obstacles in the path of the ice flow. Weertman concludes that basal water moves in sheets due to the higher water pressures generated on the near (relative to ice flow) sides of obstacles. According to Weertman, the physics of the ice hitting a bump at the bed is just as important in determining flow of basal water as the physics of the ice sliding over a bump on the downstream side (cavity formation). Weertman (1986) depends upon there being a relatively small amount of water contained in channels that are incised in the bedrock. As Kamb (1987) makes clear, this may not always be the case; orifices may play a major role in water transport.

3.2.2.2 Soft Bed

A soft bed consists of glacial till or other sediments. The situation is different from that detailed above for the following reasons.

1. The till can be eroded. This means that flowing water can incise deep channels into both the ice above and the till below.

2. The till is porous. For this reason it must be considered to be capable of carrying away a portion of the melt water.

3. The till is deformable. This would allow the till itself to be flowing and the ice to be advected by till deformation. This is an interesting perspective on

sliding that has received a great deal of attention in recent publications, and is considered in Chapter 2.36.

The first difference, having to do with how the bed can be eroded by water, has been considered by Walder (1983). He argued that for soft beds, sheet flow is unstable. If a region of the sheet of water were to become thicker, more heat would be generated, melting surrounding ice, and thickening the sheet even more. Thus the feedback is positive, producing a channelized system. Furthermore, thicker regions of water over a soft bed would exert a greater shear stress on the till, eroding the bed, and again making a thicker water layer.

In another paper on the flow of sub-glacial drainage over a soft bed (Walder and Fowler (1994)), Walder outlines the concepts developed in Walder (1983), and then continues with the analysis in a fashion similar to that used for flow over a hard bed. The issue that complicates matters greatly is that the creep of the till must be taken into account as a mechanism for channel closure. Till is also considered to be a non-Newtonian fluid, but one having very uncertain and poorly constrained properties. Walder and Fowler (1994) derive the equation

$$Q = B(\sin\alpha)^2 d^3 (P - p_c)^n. \tag{3.4}$$

Q is the discharge flux, B the ice viscosity parameter, α the ice surface slope, d the depth of the canal, P the ice overburden pressure, p_c the water pressure in the channel, and n the flow law exponent. Equation 3.4 shows that flux increases with increased water pressure, p_c. Increasing p_c make the quantity $P - p_c$ (P will remain constant on the time scales of water movement) smaller, making Q larger. Again, contrast this to the results in Equation 3.2; here smaller channels do not tend to merge with larger ones.

The idea of a porous under-layer draining away a fraction of the basal water system has been considered by several authors. Alley et al. (1986) concluded that

the mechanism is sufficient to drain away melt water formed in a particular area, but the amount of water coming from a large catchment area is too great to be drained by the till. Lingle and Brown (1987) developed a model to simulate the drainage of basal melt water by a proposed aquifer underlying Ice Stream B in West Antarctica and concluded that the pressures that result from the calculations are consistent with what is known about the system.

The creep of till as a mechanism for sliding is treated briefly in Section 2.4. This continues to be a very active area of research. What is actually happening at the ice bed interface is important to know, but as yet there is no conclusive evidence. One consideration is that regardless of the sliding mechanism (deforming till or high basal water pressures), sliding occurs in regions of basal melting. The distribution of water is also certain to play a role.

3.2.3 Summary

To quickly summarize the theoretical developments in water modeling, the following table presents some important differences in the results. Recall that a direct relation between flux and pressure indicates that the system is stable, and that inverse relations indicates that the system will move toward a dendritic network as channels come into contact.

Table 3.1: Summary of flow behaviors for englacial and basal water flow.

Location	**Type of Flow**	**Pressure to Flux**	**Authors**
Englacial	Channelized	Inverse	Shreeve (1972)
Over a hard bed	Channelized	Inverse	Hooke et al. (1990)
	Cavity and Orifice	Direct	Walder (1986)
	Sheet	Direct	Weertman (1986)
Over a soft bed	Channelized	Direct	Walder and Fowler (1994)

3.3 Data From the Field

Until now the discussion has focused on theoretical models of basal water flow. The result of most of these analyses is the flux of water and how it relates to the pressures in the basal water system. The question remains; what sort of water velocities (and fluxes) are measured in the field? A few key results are covered here.

Variegated Glacier in Alaska has been studied extensively due to its surge behavior. Some estimates of the velocity in the basal water system are around 0.025 m s^{-1} (Kamb et al. (1985)). This lower velocity is consistent with ideas about the water traveling through a complicated network of cavities and orifices. Still other velocity measurements, this time on Storglaciären in Sweden, (Seaburg et al. (1988)) indicate that the velocity is higher (0.55 m s^{-1}), and that the flow is consistent with a system of tunnels.

Both of these examples are for temperate glaciers for which the flow is both englacial and basal. In the case of the polar ice sheets, data are harder to find.

Based on oscillations in the water level of a pair of closely spaced boreholes, Kamb (2001) computes that the estimated water layer thickness under Ice Stream D is 2.5 mm. This is consistent with recent video footage of the water systems under ice streams of the Siple coast region of Antarctica. These videos were made by lowering a camera down a borehole that was created with a hot water drill. The video dramatically shows a thin layer under Ice Stream C. However, at one borehole, the depth of the water layer was determined, from video, to be closer to 1.4 *meters*. These measurements are so new that most theories about their meaning are still very speculative. Clearly they are consistent with theories about a linked cavity system.

Esker distribution in North America indicates that Walder and Fowler (1994) are probably correct in that channels in the ice only form in regions where the bed is hard. Eskers are common on the Canadian shield area where the ice sheet rested on a hard bed, but are not found on the prairies of the Midwest United states, where

the bed was soft.

Virtually all efforts to determine the pressure of sub-glacial water pressure (see Kamb (2001) for a review), indicate that the pressure in the water system is less than the ice overburden pressure. This is incorporated into the model and discussed at some length in Section 3.4.2.

If the data sound sparse, it is because they are. However good data are available for the ice surface velocities Joughin and Tulaczyk (2002). This is due to the use of satellites for collecting Synthetic Aperture Radar (SAR) images of Antarctica. Interferometric techniques can be applied to SAR data from successive satellite passes to accurately determine the surface velocity of ice. Surface velocity data are used as a basic guideline for the basal water model developed in this thesis. Basic calculations on the velocity of water in a basal water system, and the depth of that water, will be controlled by the data discussed in this section.

3.4 Water Model

When beginning the application of the above theory to a specific water model there are several factors that inform the discussion. There is no consensus on how the water flows beneath ice sheets. As the previous discussion indicates, there has been some progress in detailing the drainage systems for temperate glaciers, and there are several credible theories for the sub-glacial water systems in ice sheets. In spite of there being a number of credible theories, none have been demonstrated to be true. Progress in water modeling for ice sheets is made by careful guess work, utilizing several concepts that have their origins in the above discussion.

3.4.1 Flux Model

A flux relationship is used to model the movement of sub-basal water. The variable under consideration in this model is w, the depth of water. A flux relationship

is merely an assertion of conservation of matter for an incompressible fluid. The equation itself states that the divergence of the flux is equal to the source minus a term that accounts for transient time-dependent changes in water thickness. The flux equation, from continuity, is

$$\frac{\partial w}{\partial t} = -\nabla \cdot \vec{\sigma} + S. \tag{3.5}$$

where $\vec{\sigma} = \vec{v}w$, and $\vec{v}$ is the velocity of the water.

This is a map plane, or two dimensional model. Thus, the ∇ operator used throughout this section is defined as

$$\nabla = \frac{\partial}{\partial x}\hat{i} + \frac{\partial}{\partial y}\hat{j}. \tag{3.6}$$

Where $\hat{i}$ and $\hat{j}$ are the cardinal directions in the map plane.

The S term represents external sources of water generation. Specifically, S is the melting or re-freezing taking place at the bottom of the ice sheet. This amount is calculated using the temperature model from Section 2.3.2.

3.4.2 The Pressure Potential

Recalling Equation 3.1, it is necessary to characterize p, the pressure in the water system. The pressure of the basal water system must account for both the topography of the bedrock and the load of ice from above. The desired expression results from summing the ice overburden pressure and the effective head (with respect to sea level) of the water. An additional term N, called the effective pressure, is included to account for differences between the ice overburden pressure and the actual water pressure. This is thought of as the portion of the ice load supported by the bed, since a bump in the bed itself can rise above the water level to support the ice above it. The resulting expression for the pressure is

$$\phi = \rho_i g H + \rho_w g z_b - N. \tag{3.7}$$

Here, H is the thickness of the ice, z_b the elevation of the bed, g is the acceleration due to gravity, ρ_i and ρ_w are the densities of ice and water respectively. The effective pressure, N, is calculated with the relation given by Alley (1989a)

$$N = k_n \frac{\tau_b}{w}. \tag{3.8}$$

With k_n a parameter, and τ_b, the driving stress.

Equation 3.8 represents the simplest expression of the intuitive ideas that increased τ_b will result in increased effective pressure, and that higher pressure tends to spread out a basal water system, or decrease the water thickness. The concept is thoroughly treated in Alley (1989b) and Alley et al. (1989).

The expression for pressure is further simplified by noting that the ice thickness, H, can be written as the difference between surface elevation, h and bed elevation z_b. Furthermore, if the driving stress is assumed to be balanced locally by vertical shear stresses, it can be written as

$$\tau_b = \rho_i g H |\nabla h|. \tag{3.9}$$

The result of the simplification is

$$\phi = \rho_i g h + \rho_i g (\frac{\rho_w}{\rho_i} - 1) z_b - k_n \frac{\rho_i g (h - z_b) |\nabla h|}{w}. \tag{3.10}$$

Or, using known values for the densities and simplifying:

$$\phi = \rho_i g \left(h + 0.09 z_b - k_n \frac{(h - z_b) |\nabla h|}{w} \right). \tag{3.11}$$

Equation 3.11 highlights the fact that when determining the direction of basal water flow with $\nabla \phi$, the ice surface slope is approximately ten times more important than the bed slope.

3.4.3 The Water Velocity

Equation 3.5 is a continuity equation defining flow in a basal water system. Before this equation can be solved for the water thickness, the velocity must be specified in terms of the pressure gradient. This is one of the most challenging aspects of the model. It is here that a complex basal drainage network is averaged into a single velocity. It is clear from the review of the literature that there is little consensus on what is really happening in these basal drainage systems. It is also clear that the constructs at hand are not appropriate for the large grid cell discretization scheme that will be used for the ice sheet model.

To address these problems, begin from first principles. Consider the flow of water in a conduit of arbitrary shape, but uniform cross section, subject to the pressure potential described in the previous section. The area of the conduit's cross section is denoted A_g, its perimeter, P_g, and the conduit's length, L.

Assume that the fluid in this conduit is in equilibrium–the sum of stresses on the fluid is zero. The primary stresses acting on the fluid are the shear stresses due to motion of fluid along walls, denoted τ_w, and the stresses arising from the pressure potential gradient. Viscous forces are assumed negligible in comparison. The equilibrium between the stresses is expressed

$$A_g L \nabla\phi = P_g L \tau_w. \tag{3.12}$$

Solving for τ_w gives

$$\tau_w = \frac{A_g}{P_g}\nabla\phi \tag{3.13}$$

To continue, introduce the non-dimensional Darcy friction factor (Schetz and Fuhs, 1996),

$$f = \frac{2D}{\rho_w v^2}\frac{\Delta p}{L}, \tag{3.14}$$

v is the velocity, Δp is the pressure drop in length L, D is 4 times cross sectional

area, A_g, divided by perimeter, P_g

$$D = \frac{4A_g}{P_g}. \tag{3.15}$$

Notice that in this case the change in pressure per unit length is equal to the gradient of the previously defined pressure potential

$$\frac{\Delta p}{L} = \nabla\phi. \tag{3.16}$$

Rearranging 3.14, and making use of the Equations 3.15 and 3.16 gives

$$\tau_w = \frac{A_g}{P_g}\nabla\phi = \frac{f\rho_w v^2}{8}. \tag{3.17}$$

The ratio $\frac{A_g}{P_g}$ is called the hydraulic radius and denoted R. The velocity can be solved for, giving

$$\vec{v} = \left(\frac{8}{f\rho_w}\right)^{\frac{1}{2}} [R\nabla\phi]^{\frac{1}{2}} \tag{3.18}$$

where the direction of the vector quantity $\vec{v}$ will be the same as the direction of $\nabla\phi$.

This expression and its derivation are interesting because they yield the velocity as a function of the potential, which is exactly what is needed to complete the continuity Equation 3.5. The development follows that of the *Chézy (1768)* for uniform channel flow.

There are obvious shortcomings to this approach. When converting between the course gridding of a numerical model, and the theoretical constructs developed by others, a single conduit is not appropriate. Rather, a set of parameters should be introduced that indicate the fraction of a grid cell that is occupied by water and how much the path of that water deviates from the direction defined by the potential gradient. This latter parameter indicates that while on a gross scale water will flow down the gradient, on a small scale it could be moving in any direction. This parameter is called the tortuosity. If both parameters are introduced early in the derivation, when balancing stresses, the result would be the same in its exponential form, differing instead in the constant term.

Clearly, a more general form of Equation 3.18 is needed. The exercise of deriving it is instructive in that it demonstrates how an estimate might be found based on a simple balance of stresses.

For practical purposes, it is convenient to use the equation developed by Robert Manning (Schetz and Fuhs (1996)). This power law correlation simplifies Equation 3.18 and fits experimental data very nicely.

$$\vec{v} = \frac{1}{n'} [R]^{\frac{2}{3}} \left[\frac{\nabla \phi}{\rho_w g} \right]^{\frac{1}{2}} \tag{3.19}$$

Note that the pressure gradient divided by $\rho_w g$ is unitless. Also note that it is the direction of the pressure gradient that determines the direction of flow. Equation 3.19 can be written as follows to emphasize the direction of flow

$$\vec{v} = \frac{1}{n'} [R]^{\frac{2}{3}} \frac{\nabla \phi}{(\rho_w g |\nabla \phi|)^{\frac{1}{2}}} \tag{3.20}$$

The value of the Manning coefficient for basal water systems is open to speculation. To help guide inquiry, Table 3.4.3 presents some known values of n' for open channel flow. The units of n' are $\mathrm{m}^{-\frac{1}{3}}\mathrm{s}$. The values in the table are interesting because they obviously represent some gross parameterization of small scale phenomena that are very complicated. Take the case of heavy brush for example. Clearly the tortuosity for such flow is very large, but the equation and roughness coefficient appear to give accurate results.

A final extension to the Manning equation can be made. By allowing freedom over the choice of exponents, the model should be able to handle many more flow regimes. These exponents are known to be sensitive to changes between laminar and turbulent flow (Schetz and Fuhs (1996)). Because the conditions under ice sheets are uncertain, the exponents are treated as parameters. The resulting equation is written

$$\vec{v} = \frac{1}{n'} R^p \left[\frac{\nabla \phi}{\rho_w g} \right]^q . \tag{3.21}$$

Table 3.2: Some values of the Manning roughness coefficient.

Channel Type	n'	**Uncertainty**
Artificially Lined:		
Glass	0.010	0.002
Finished Cement	0.012	0.002
Corrugated Metal	0.022	0.005
Excavated Earth:		
Gravelly	0.025	0.005
Stone Cobbles	0.035	0.010
Natural Channels:		
Clean, straight	0.030	0.005
Major Rivers	0.035	0.010
Flood plains:		
Light Brush	0.05	0.02
Heavy Brush	0.075	0.025

In Chapter 4 the exponents are fixed at values that are consistent with laminar sheet flow. In Chapter 5 they are allowed to carry based on a simple scheme to determine if flow is laminar or turbulent.

An appropriate parameterization of the basal flow can be obtained from Equation 3.21, provided that suitable values of p, q, and n' can be determined with sensitivity studies. Applying this approach, Alley (1996) used a similar scheme to model mountain glaciers through a range of externally produced pressures to give reasonable non-steady responses. Further support of this approach is delivered by considering the equation describing the laminar flow of water between parallel plates used by Weertman (1972),

$$\vec{v}_p = \frac{w^2 \nabla \phi}{12\mu} \tag{3.22}$$

where μ is the viscosity of water, and $\vec{v}_p$ the velocity of the water. Equation 3.22 can be arrived at from a particular parameterization of Equation 3.21 (p=2, q=1, and appropriate n'). Basal water systems exhibiting sheet or distributed flow may be much larger than tens of meters (Kamb (1991) and Weertman (1986)). A final argument for the use of Equation 3.21 is provided by flood plain modelers, who

Table 3.3: Parameters used in velocity expressions.

Flow Regime	p	q	n'	R
Laminar	2	1	0.02	$\frac{w}{2}$
Turbulent	$\frac{2}{3}$	$\frac{1}{2}$	0.08	$\approx \frac{w}{20}$

routinely use the Manning equation to model phenomena that take place on very large scales (Bedient and Huber (2001) and Schetz and Fuhs (1996)).

3.4.4 Specifying the Parameters

Some reasonable values for p, q, n', and R are summarized in Table 3.4.4. The two basic regimes for flow are laminar and turbulent. Laminar flow is represented by Equation 3.22, the result for laminar flow between parallel plates. For turbulent flow, the general Manning equation with appropriate n' is used. In reality, flow is probably somewhere between these two; the possibilities will be explored in the next chapter.

Depending upon the actual flow system, R can vary over a wide range of values. The simplest estimate for values of R uses a square cell with side L and uniform water depth w. The area over the perimeter is then $\frac{wL}{2L+2w}$. Because for our modeling scheme $L >> w$, $R \approx \frac{w}{2}$. However, because R is the area wetted divided by the perimeter, R is expected to fall off quite rapidly as the complexity of the drainage system increases. This is because the area is going to be more or less fixed, most of the cell has water at its base, but the perimeter is a function of tortuosity of the system.

A simple assumption that can be applied in water modeling is that for water layer thickness of less than one centimeter, the flow is expected to be closer to laminar, and a sheet flow scheme should be used. For water layer thickness greater than 1 cm, the flow is turbulent, and the Manning scheme should be used. This concept is applied to the experiments in Chapter 5.

Finally, on small scale the value of R for sheet flow is clearly $w/2$. However, in a model in which the scale is very large, R becomes a parameterization of the tortuosity of the drainage system, just as it is for the turbulent flow.

3.4.5 Estimating Fluxes and the Contribution of an Aquifer

Now that a framework has been established, some simple computations can be done to find the amount of water various drainage schemes are capable of draining. From the review of previous work, it is clear that aquifers do not play a major role in the drainage of basal water. The calculations here will highlight that, and estimate a fraction of water that is drained by the aquifer, a variable that does appear in the water model.

The velocities and annual discharge flux per square cell, Q, will be computed for:

1. Thin film of water. Velocity determined by Equation 3.22.
2. Channelized system. Velocity from Manning Equation 3.21. $R = \frac{w}{20}$.
3. Saturated aquifer. Velocity from Darcy's law.

The final case, computing the discharge with Darcian flow is determined by Darcy's Law, given by (Schetz and Fuhs, 1996)

$$\vec{v} = k_D \left(\frac{\nabla \phi}{\rho_w g} \right). \tag{3.23}$$

Where k_D is the hydraulic conductivity of the material.

Assumptions made about the nature of the aquifer and other variables are given in the Table 3.4.5. These values, particularly those used for the aquifer, are consistent with those give in Paterson (1994a). Results of a quick calculation appear in Table 3.5.

Typical meltwater productions in Antarctica are of the order of 1 mm per year. Taken over an area of 25 km^2 this is going to be 2.5×10^5 m^3/y. Both the sheet

Table 3.4: Values used in flow calculations.

Variable	**Symbol**	**Value**
Grid size	L	5 km
Pressure gradient	$\|\nabla\phi\|$	$10\ \frac{Pa}{m}$
Thickness of water layer	w	2.5 mm
Viscosity of water	η	$1.8 \times 10^{-3} Pa \cdot s$
Acceleration due to gravity	g	$9.8 \frac{m}{s^2}$
Density of fresh water	ρ_w	$10^3 \frac{kg}{m^3}$
Thickness of an aquifer	T	$10m$
Hydraulic conductivity of aquifer	k_D	$1.1\times\ 10^6$ m/s
Manning coefficient	n'	$.08 m^{-1/3} s$
Hydraulic Radius	R	$\frac{w}{20}$
Seconds in a year	SY	$3.154 \times 10^7 s/y$

Table 3.5: Flow velocities and volumes for three different flow types.

Flow Model	**Equation**	v	Q
Sheet flow, parallel plate.	$v = \frac{w^2 \|\nabla\phi\|}{12\eta}$	2.9×10^{-3} m/s	1.1×10^6 m^3/y
Manning	$v = \frac{1}{n'} R^{\frac{2}{3}} (\frac{\|\nabla\phi\|}{\rho_w g})^{\frac{1}{2}}$	1.0×10^{-3} m/s	3.9×10^5 m^3/y
Aquifer, Darcy.	$v = k \frac{\|\nabla\phi\|}{\rho_w g}$	1.0×10^{-9} m/s	1.8×10^2 m^3/y

flow and Manning flow values are capable of completely draining this melt water production.

Table 3.5 shows that the aquifer system is not adequate to drain typical melt water productions. However, the aquifer can drain a fraction of the meltwater that is being produced. The fraction that can be drained will clearly depend on the nature and extent of the tills that constitute the aquifer, as well as the amount of melt water production. As a simple modeling technique, a drainage parameter is introduced that drains a constant amount of the water present into an aquifer. It is discussed further in Section 4.3.2. Based on the simple calculations above, it appears that about 1% is a reasonable amount of drainage. That being said, this drainage parameter varies over some range, as there is really little known about the nature of the till. General results show that glacial tills can have hydraulic conductivities that range over 3 orders of magnitude. If the till is sandy in nature, the range is even larger.

It is also interesting to consider the graph in Figure 3.4.5. The curves were generated by considering the values of velocity produced by the previous table. The graph shows that the sheet flow velocity of Equation 3.22 quickly exceeds the velocities of Equation 3.19. This is reasonable as we do not expect sheet flow to extend beyond water layer thicknesses of about 10 mm. The actual velocities are comparable to those described in Section 3.3. They do range a bit lower (factor of 5 or more), which is to be expected, considering that the water layer thickness is thin compared to temperate glaciers and the complexity of drainage systems beneath ice sheets is much more complex than that found under temperate glaciers (where the velocity data are taken). In practice the velocities may be even lower due to very high tortuosities.

3.5 The Finite Element Approach

The components of the model are the flux equation (Equation 3.5), the pressure potential equation (Equation 3.11) and the Manning velocity equation (Equation

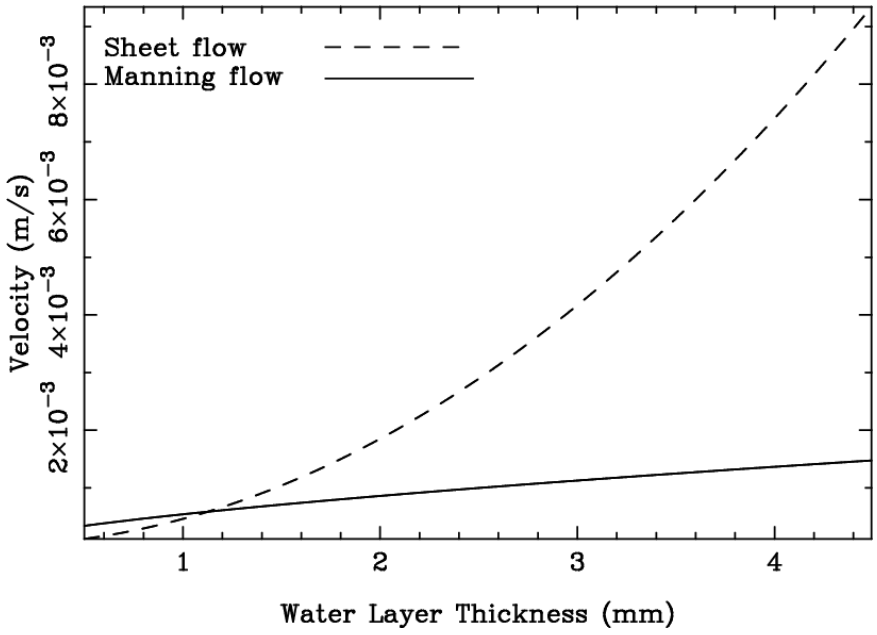

Figure 3.2: Graph compares the velocities from Manning (Equation 3.19) and Sheet flow (Equation 3.22)

.

3.21). These components are now assembled into a single differential equation that is solved numerically with the finite element method. The creation of the differential equation and the technique for solving it follow.

3.5.1 A Differential Equation for Water Depth

Begin with Equation 3.5

$$\frac{\partial w}{\partial t} = -\nabla \cdot \vec{\sigma} + S. \tag{3.24}$$

Substitute Equation 3.21 to give a differential equation in terms of water thickness and pressure gradients

$$\frac{\partial w}{\partial t} = -\nabla \cdot \left(w \frac{1}{n'} R^p \left[\frac{\nabla \phi}{\rho_w g} \right]^q \right) + S. \tag{3.25}$$

A general form of the hydraulic radius can be written as

$$R = \frac{w}{c_R}. \tag{3.26}$$

This form allows for the tortuosity to be expressed with c_R.

In order to simplify, identify the set of constants as γ:

$$\gamma = \frac{1}{n' c_R^p (\rho_w g)^q}. \tag{3.27}$$

Introducing γ and substituting for R makes the flux equation read

$$\frac{\partial w}{\partial t} = -\gamma \nabla \cdot \left(w^{p+1} \left[\nabla \phi \right]^q \right) + S. \tag{3.28}$$

This is a differential equation in terms of w. Solving it will yield the water distribution under the ice sheet at some specified time.

3.5.2 The Weak Formulation

The differential Equation 3.28 will not be solved in its present form. Instead, recast the equation into the weak form by collecting all terms on the left hand side, multiplying by an arbitrary weighting function, and integrating over the domain of the problem. This formulation of a differential equation is the starting point in finite element analysis. There are many excellent textbooks detailing the finite element method. One such reference is Becker et al. (1981).

Let the weighting functions be given by v, the domain of the problem by Ω, and an infinitesimal element of the two dimensional domain dA. The weak formulation is given by

$$\iint_\Omega \left[v \frac{\partial w}{\partial t} + v\gamma \nabla \cdot \left(w^{p+1} \left[\nabla \phi \right]^q \right) - vS \right] dA = 0 \tag{3.29}$$

To simplify, introduce

$$k = w^p |\nabla \phi|^{q-1} \tag{3.30}$$

and write

$$\iint_{\Omega} \left[v\frac{\partial w}{\partial t} + v\gamma\nabla \cdot (kw\nabla\phi) - vS \right] dA = 0 \tag{3.31}$$

This form is convenient as it groups all w dependence into the single term ,k and makes the direction of flow explicit by leaving a single power of $\nabla\phi$.

Note that application of the chain rule yields

$$\nabla \cdot (vkw\nabla\phi) = kw\nabla\phi \cdot \nabla v + v\nabla \cdot (kw\nabla\phi). \tag{3.32}$$

Rearranging gives

$$v\nabla \cdot (kw\nabla\phi) = \nabla \cdot (vkw\nabla\phi) - kw\nabla\phi \cdot \nabla v. \tag{3.33}$$

Which can be substituted for the second term of the integrand of Equation 3.31, giving

$$\iint_{\Omega} \left[v\frac{\partial w}{\partial t} + \gamma\nabla \cdot (vkw\nabla\phi) - \gamma kw\nabla\phi \cdot \nabla v - vS \right] dA = 0. \tag{3.34}$$

The divergence theorem can be applied to the second term of the integrand of Equation 3.34 to give

$$\iint_{\Omega} \gamma\nabla \cdot (vkw\nabla\phi) dA = \gamma \iint_{\partial\Omega} kw\frac{\partial\phi}{\partial n} v ds. \tag{3.35}$$

Here $\partial\Omega$ has been introduced to represent the boundary of the region Ω and n represents the direction that is normal to the boundary $\partial\Omega$.

Physically, this integral represents the flux of water into or out of the region Ω. The boundary term is either used to specify a known flux across a boundary or set to zero by judiciously selecting weighting functions such that v is equal to zero everywhere on $\partial\Omega$.

Thus, neglecting the boundary term, the final expression for the weak formulation is

$$\iint_{\Omega} \left[v\frac{\partial w}{\partial t} - \gamma kw\nabla\phi \cdot \nabla v - vS \right] dA = 0. \tag{3.36}$$

3.5.3 The Galerkin Approximation

At this point an approximation scheme is introduced for solution of the equation on computer. Solutions are assumed to be representable by finite sums of basis functions.

$$w \approx \sum_i w_i \psi_i \tag{3.37}$$

$$v \approx \sum_j v_j \psi_j \tag{3.38}$$

where ψ represents a suitable, complete set of basis functions. These basis functions have the property that they give a value of one at exactly one nodal point and a value of zero at all others. More detailed discussion on this approximation scheme and the choice of basis functions appears in Becker et al. (1981). The positions of w_i and v_j will correspond to the nodal points in a finite element mesh.

The series approximations of Equation 3.37 and 3.38 are substituted into 3.36 and k is written explicitly to give

$$\sum_i \sum_j w_i v_j \iint_\Omega \left[\psi_j \frac{\partial \psi_i}{\partial t} - \gamma k \psi_i \nabla\phi \cdot \nabla\psi_j - \psi_j S \psi_j \right] dA = 0. \tag{3.39}$$

From the above expression the following terms can be identified by exploiting the freedom in arbitrary v_i. Choose v_i=1 when $i = j$ and $v_i = 0$ elsewhere.

$$K_{ij} = -\gamma \iint_\Omega k \psi_i \nabla\phi \cdot \nabla\psi_j dA \tag{3.40}$$

$$f_j = \iint_\Omega S \psi_j dA \tag{3.41}$$

Assuming that a suitable time stepping scheme can be applied to the $\frac{\partial w}{\partial t}$ term, at each time step the problem reduces to the following matrix equation:

$$\mathbb{K}\vec{x} = \vec{f} \tag{3.42}$$

where the vector x is the solution vector containing the w_i for each node in the finite element mesh.

CHAPTER 8

CONCLUSIONS

8.1 Achievements

Several important achievements have resulted from the development of a basal water model. They are itemized below.

- The reproduction of the system of Ross Ice Streams was accomplished in Chapter 4. The system resulting from the model includes a very strong match to Ice Stream D and Ice Stream E. A stagnant Ice Stream C is evidenced, which is what is expected from Retzlaff and Bentley (1993). There is a good showing from Whillans Ice Stream (Ice Stream B), and an under-stated Ice Stream A. The overall shape of each of the Ross Ice Streams was remarkably similar to what has been measured by InSAR, including the upstream areas and tributaries. There was some evidence of water piracy from the upstream areas of Ice Stream C into both Ice Stream D and Whillans Ice Stream.

- The water model has been shown to offer a real advantage over simpler, but commonly used, modeling schemes. Chapter 5 demonstrates that proper treatment of the basal water system will offer a much more reasonable development of a large scale glaciation scenario, as well as a closer match to data on global sea level change.

- The prediction of sub-basal lakes is possible by coupling the water model with an algorithm that seeks out depressions in a potential field. All major lakes in Antarctica have been identified with this method, and Chapter 6 shows that the agreement with field observations is good. Several lakes that have not been

identified in the field can be predicted in this manner.

- Sub-glacial lakes can be evaluated for their stability by considering surface slopes of the ice sitting on top of them. The water sub-glacial lakes are capable of releasing or absorbing will have a significant impact the basal water system.

8.2 Warts and All

In working with the water model a number of shortcomings of the approach become apparent. They are spelled out here for clarity. Many of them do not represent shortcomings of the water model per se, but rather shortcomings of the ice sheet model (and in many cases, ice sheet models in general).

- The different time scales are difficult to reconcile. The water moves quickly and the ice moves slowly. A model for both has to take a snap shot of the ice distribution, and then allow the water distribution to reach steady state. This works most of the time, however, there are physically valid regions of parameter space where instability becomes an issue. This should not be the case.

- In addition to different time scales, there are also different spacial scales. The entire theoretical framework for basal water is formulated in terms of features that are tens of meters. Modeling at that scale is not currently a possibility. Much of the work here has been adapting the appropriate mapping from small scale features to large ice sheet model grid sizes.

- To develop a system of ice streams with the model, an initialization sequence must be run. This sequence is essential, it creates the temperature distribution of the ice sheet. The initialization sequence has a significant impact on the state of the ice sheet. Figure 4.9 shows the impact of initialization on the surface elevation. Figure 4.20 shows the driving stresses resulting from the initialization sequence. Results such as these cast doubt on the validity of modeling results.

- The water layer thickness appears to be deeper than data would lead one to think it should be. Modeling results consistently show a depth of water approaching one cm near the grounding line. Raising the drainage parameter will help this, but there are not presently physical grounds for doing so. Data indicate that depths of about 2 or 3 mm are reasonable.

- Is a conservation model for basal water the right approach? In modeling it became clear that there is a great deal of uncertainty in the pressures of the basal water system. Perhaps a better approach would be to develop a differential equation in terms of the pressure, solve it, then consider basal water and its velocity.

- The lack of horizontal advection in the temperature model is a problem. Horizontal advection represents a significant heat source in the case of ice streams.

- The lack of an ice shelf model makes the grounding line conditions a heuristic at best.

- The absence of longitudinal stresses in the ice streams makes the ice sheet profiles generated by the model unrealistic. Furthermore, longitudinal stresses play an important role in other aspects of ice stream dynamics and ice flattening over lakes. Thus, in the long term, their inclusion will be essential.

8.3 Future Work

There are important extensions that can be made to this work on basal water. Each of the following is an important research project that the work done in this thesis will make possible.

- A detailed investigation of the relation between the relatively small scale features that are the known mechanisms for basal water discharge (detailed in

Chapter 3), and the necessity of larger grid sizes in ice sheet models. In other words, more efforts at achieving better parameterizations in the water model.

- A comparison of the sliding characteristics of rock-floored ice streams and sediment-floored ice streams would provide important insights into a wider range of fast flowing ice. The studies of Chapter 4 and Chapter 5 used an assumption of uniform basal conditions in terms of the substance under the ice sheets. The assumption was that the material was some sort of till. There are many important glaciers, such as the Byrd Glacier, that are rock floored, and the approach to them should be different. The most significant difference would be the greatly reduced drainage parameter, as there is no longer a permeable layer of till beneath.

- Further analysis of the stability of sub-glacial lakes will complete the work initiated in Chapter 7. The great unanswered question of Chapter 7 is the time scales over which the lakes deliver their water to the drainage system. This is a great glacial dynamics problem. It involves the longitudinal forces of ice over a lake, the boundary conditions of the ice sliding into and out of the lake region, and the buttressing of the ice around the lake.

- Improving the model's thermal dynamics to include advective heat transfer. This will produce much more realistic temperature profiles in the region of the ice streams.

- A study of the feedback between basal water and various other important ice sheet variables. For instance, now that it has been established that the Ross Ice Streams have a net positive mass balance (Joughin and Tulaczyk, 2002), the water model can be used to determine how long this positive mass balance can exist before the sliding increases.

- Very high resolution water modeling done with bathymetry of the Amundsen Sea floor. This bathymetry represents a pristine deglaciated bed. Putting an ice sheet over it will allow for an investigation of phenomena that are finer in resolution than current, Antarctic data sets allow.